

Principles in the design of ligand-targeted cancer therapeutics and imaging agents

Madduri Srinivasarao, Chris V. Galliford and Philip S. Low

Abstract | Most cancer drugs are designed to interfere with one or more events in cell proliferation or survival. As healthy cells may also need to proliferate and avoid apoptosis, anticancer agents can be toxic to such cells. To minimize these toxicities, strategies have been developed wherein the therapeutic agent is targeted to tumour cells through conjugation to a tumour-cell-specific small-molecule ligand, thereby reducing delivery to normal cells and the associated collateral toxicity. This Review describes the major principles in the design of ligand-targeted drugs and provides an overview of ligand–drug conjugates and ligand–imaging-agent conjugates that are currently in development.

Ligand–drug conjugates
Receptor-targeted drugs that are conjugated, typically via chemical linkers, to non-peptide, low-molecular-weight targeting ligands.

Internalization
Receptor-mediated endocytosis of the conjugate inside the cell.

A rapidly growing class of anticancer drugs uses a targeting moiety to deliver a potent (but typically nonspecific) cytotoxic agent selectively to malignant cells¹. The general structure of this class of drugs involves a targeting moiety linked to a therapeutic payload via a spacer that often contains a cleavable bond (FIG. 1). Although the therapeutic component may be similar among members of this class of drugs, a wide variety of targeting moieties have been used, and antibodies^{2,3}, aptamers^{4–6}, small protein scaffolds⁷, peptides^{8–11} and low-molecular-weight non-peptidic ligands^{12–16} are all attracting considerable attention. Antibody–drug conjugates (ADCs) have had the greatest success to date^{17–19}, with two ADCs (trastuzumab emtansine²⁰ and brentuximab vedotin²¹) already on the market and many more in clinical trials. However, the recent clinical development of multiple low-molecular-weight non-peptidic ligand–drug conjugates (vintafolide, etarfolatide, EC1456 and EC1669), together with the intense research focused on aptamer-, scaffold- and peptide-targeted drugs²², suggests that these smaller targeted conjugates could be poised for similar success.

In this Review, we focus on the smaller ligand-targeted drugs, as they differ markedly (and often advantageously) in their pharmacokinetics⁸, antigenicity^{23,24}, *in vivo* and *in vitro* stability²⁵, conjugation chemistry^{26,27}, ease and cost of manufacturing²⁸, and ability to penetrate solid tumours^{29–35} compared with their larger, more complex counterparts. We summarize the criteria for the effective design and development of low-molecular-weight ligand-targeted cancer therapeutics and, in particular, address the principles that influence

selection of the targeted receptor, design of the targeting ligand and optimization of the therapeutic payload. We also discuss the linker chemistry for tethering a ligand to its therapeutic payload and possible linker-cleavage strategies for the selective release of the payload after endocytosis by malignant cells. Finally, we review the ligand–drug conjugates and ligand–imaging-agent conjugates that are in preclinical development and in clinical trials.

Tumour-specific receptor selection

The approval of a drug by the US Food and Drug Administration (FDA) or other regulatory agency is primarily determined by its efficacy and safety. For ligand–drug conjugates, efficacy is predominantly controlled by the potency of the conjugate's therapeutic payload and the number of receptors available to mediate drug internalization by cancer cells. Safety is governed by the specificity of the targeted conjugate for cancer cells compared with normal cells. As the safety aspect depends on the biodistribution and location of the receptors to which the conjugate binds, careful selection of the cancer cell receptor is essential to minimize conjugate toxicity.

Level of cancer-specific receptor expression. To be useful for targeted drug delivery, the targeted receptor must generally meet two criteria: it must be overexpressed on cancer cells relative to normal cells^{36,37}, and its absolute level of expression on cancer cells must be sufficient to enable delivery of therapeutic quantities of the desired drug by receptor-mediated endocytosis.

Department of Chemistry,
720 Clinic Drive, Purdue
University, West Lafayette,
Indiana 47907, USA.
Correspondence to P.S.L.
e-mail: plow@purdue.edu
doi:10.1038/nrd4519
Published online
20 February 2015

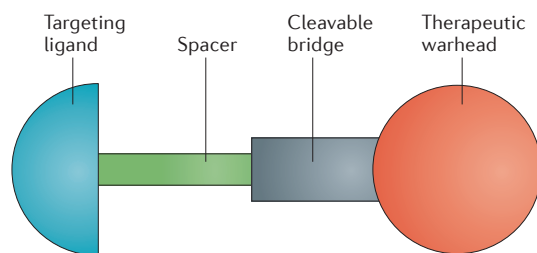


Figure 1 | Schematic of a typical ligand–drug conjugate. The design of ligand-targeted therapeutic agents commonly includes: a targeting ligand; a spacer; a cleavable bridge that is stable in circulation but that permits drug release following endocytosis into a target cell; and a therapeutic ‘warhead’. Conversely, ligand-targeted imaging agents generally do not contain a cleavable bridge, and the payload consists of an imaging, rather than a therapeutic, agent.

Regarding receptor overexpression relative to normal cells, a threefold overexpression of the targeted receptor on the cancer cell is generally considered to be sufficient to warrant further investigation, although greater upregulation is preferred. The reasons for this assessment are as follows. First, delivery of even threefold more of a drug into a malignant cell than into a healthy cell is a substantial improvement compared with the corresponding non-targeted therapy¹². Second, many normal tissues are relatively non-mitotic and are therefore less sensitive to antimitotic chemotherapeutic agents than are cancer cells³⁸. Third, the receptor recycling rate is often greater in malignant cells than in healthy cells^{39,40}, allowing a similar receptor abundance to translate into increased drug delivery in cancer cells. Finally, many of the more prominent receptors that are currently targeted by drugs in the clinic are expressed in only twofold to threefold excess in malignant tissues. For example, the receptor tyrosine protein kinase ERBB2 (also known as HER2) is expressed in only twofold excess in breast cancer relative to normal tissue⁴¹, whereas CD30 is expressed in 3.3-fold and 4.4-fold excess in Hodgkin’s lymphoma⁴² and anaplastic large cell lymphoma⁴³, respectively. Transmembrane protein NMB is similarly present in fourfold excess in melanoma relative to healthy tissue^{44,45}. Other examples of receptors that are commonly overexpressed in certain types of cancer include hepatocyte growth factor receptor (encoded by *MET*)^{46,47}, luteinizing hormone-releasing hormone receptor⁴⁸ and epidermal growth factor (EGF) receptor⁴⁹.

In addition to the desired overexpression of the targeted receptor on cancer cells, a minimal absolute level of receptor expression is required. Therefore, if one plans to deliver a drug with a median inhibitory concentration (IC_{50}) of 10 nM into a cancer cell to induce tumour regression, the intracellular concentration of drug might need to be sustained at 30 nM to promote quantitative tumour cell death. Assuming an average cancer cell diameter of 20 μm , one can estimate an intracellular volume of $\sim 4,000 \mu\text{m}^3$, suggesting that $\sim 72,000$ molecules must be maintained within the cancer cell to achieve the desired steady-state concentration of 30 nM. Assuming

that 3 molecules can be delivered by each receptor per day³⁹, achievement of a therapeutic dose would require at least 24,000 receptors per cell, as long as there is no loss of drug due to metabolism or excretion during this period. Common tumour-enriched antigens, such as folate receptor (FR)⁵⁰, prostate-specific membrane antigen (PSMA; also known as FOLH1)⁵¹ and glucose transporter 1 (GLUT1; also known as SLC2A1)⁵², are often expressed in vast excess of this threshold receptor density. For example, the level of FR type α (FR α) expression may be as high as 2.8 million receptors per cancer cell^{53,54}. Although PSMA is expressed at lower levels, many prostate cancers, including the LNCaP (PSMA⁺) prostate cancer cell line, express in excess of one million receptors per cell⁵⁵. Other receptors that may be present in sufficient quantities on cancer cells to be useful for targeted drug delivery include somatostatin receptor 2 (SSTR2)^{56–58}, cholecystikinin type B receptor (CCKBR)^{59–61}, bombesin receptor^{62–64}, and sigma non-opioid intracellular receptor 1 (SIGMAR1) and SIGMAR2 (REFS. 65–69). Moreover, several cell-adhesion proteins⁷⁰, such as intercellular adhesion molecule 1 (ICAM1; also known as CD54)^{71–73}, leukocyte function-associated antigen 1 (LFA1; also known as ITGB2)⁷⁴ and CD24 (REF. 75), are overexpressed on some tumours, for which they have notable potential for use in ligand-targeted therapies⁷¹.

Internalization and rate of receptor recycling. In receptor-mediated drug delivery, the ligand–drug conjugate will commonly enter its target cell by receptor-mediated endocytosis^{76–78} and then traffic to an intracellular compartment such as a recycling endosome, a compartment of uncoupling of receptor and ligand (CURL) or a lysosome. Within a CURL, the conjugate and receptor may dissociate from one another and sort into separate intracellular compartments⁷⁹, allowing the receptor to be either degraded or returned to the cell surface for another round of endocytosis³⁹ (FIG. 2).

As the availability of empty receptors on the plasma membrane will depend on the rate of return of unoccupied receptors from intracellular endosomes, an ideal receptor will be one that either recycles frequently or is resynthesized rapidly following degradation. Examples of receptors that meet these requirements include EGF receptor⁸⁰, PSMA and FR α ⁵⁴. Recycling rates and resynthesis rates may vary among receptors and cell types, so each must be separately analysed for every pathologic tissue⁵⁴. An assessment of the rate of receptor replenishment on the cell surface is crucial, as any drug that is administered more frequently than the rate of reappearance of empty receptors at the cell surface will cause unnecessary toxicity³⁹.

Although the internalization of the targeted receptor is helpful to achieve a desired therapeutic effect, it is not always necessary. For example, Z-360 is an orally deliverable CCKBR antagonist that has been used to target imaging agents and therapeutic agents to tumours that overexpress CCKBR⁸¹. Like most other antagonists, Z-360 is not endocytosed; nevertheless, successful therapy has been observed owing to the high tumour-specific expression of CCKBR that resulted in

Receptor overexpression

The high expression level of a receptor in one tissue relative to other tissues (for example, in tumours versus healthy cells).

Receptor recycling rate

The rate at which a surface receptor internalizes and then returns to the cell surface.

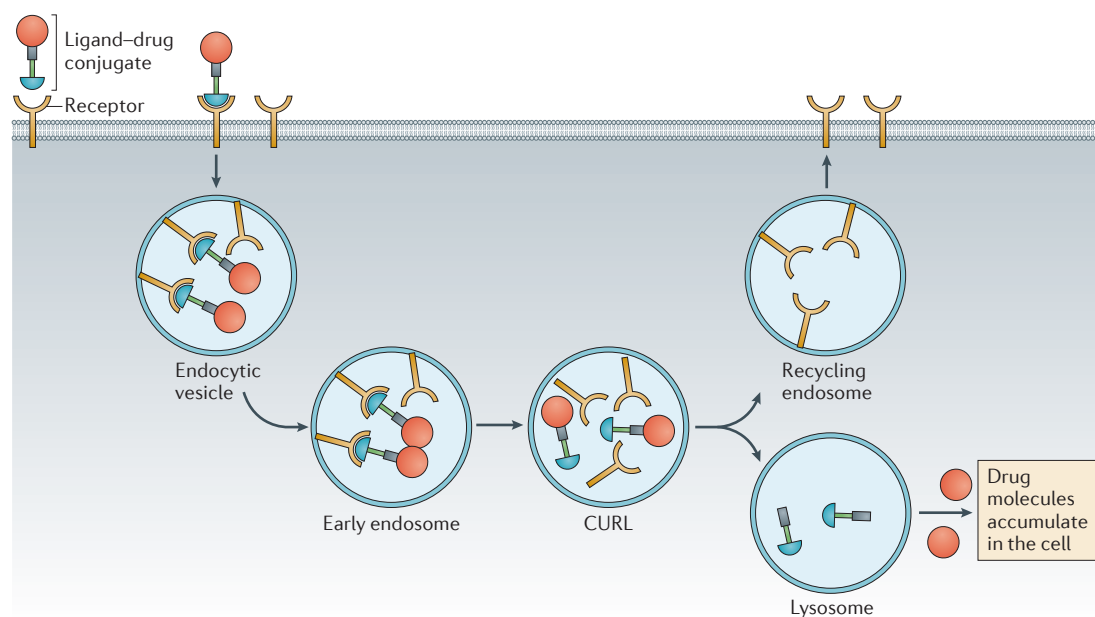


Figure 2 | **Ligand–drug conjugate entry into the cell.** Following endocytosis, ligand–drug conjugates may be trafficked through different intracellular compartments, depending on the receptor that is exploited for the internalization of the conjugate. Some of the more common compartments that are encountered during intracellular trafficking include: early endosomes; compartments for uncoupling of receptor and ligand (CURLs), where dissociation of the conjugate from the receptor may occur; recycling endosomes, which can deliver the internalized receptor back to the cell surface; and lysosomes, where the receptor and the conjugate can be degraded.

the concentration of the conjugate on all malignant cell surfaces⁸². Therefore, a non-internalizing receptor-targeted drug will still accumulate in the diseased tissue if three conditions are met. First, the targeted receptor must be enriched in the diseased tissue. Second, the therapeutic ‘warhead’, post-cleavage, must be released from the targeting ligand at the cell surface without requiring entry into the target cell. Finally, the size of the cluster of pathologic cells must be sufficient to ensure that any drug that is released from one pathologic cell would have to diffuse past many other pathologic cells before it could leave the tumour mass. These three criteria will certainly be met in many solid tumours, where extracellular hydrolytic enzymes such as matrix metalloproteinase 2 (MMP2) and MMP9 (REFS 83,84) can be exploited for enzymatic drug release and where malignant lesions can be millions of cell layers thick.

Location and accessibility of receptor. An ideal target receptor will generally be expressed on the surface of a cancer cell and not within its cytoplasm or nucleus. Although expression data on intracellular receptors (such as steroid receptors and retinoic acid receptors) may reveal that such receptors are upregulated in pathologic cells^{85,86}, ligand–drug conjugates that target these intracellular receptors must be nonspecifically permeable to cell membranes in order to have access to them. Such conjugates will obviously also enter healthy cells, where they may encounter similar conditions that promote drug release, causing unwanted damage to the healthy tissues. Moreover, as the volumes of distribution for drug conjugates that must diffuse passively across

plasma membranes to find their intracellular receptors will necessarily include receptor-negative cells, higher concentrations of conjugate will have to be administered to achieve an effective dose. By contrast, ligand–drug conjugates that target cell surface receptors can be designed to be membrane-impermeable, ensuring that only cells with the appropriate cell surface receptors can promote their uptake.

Receptors that are normally expressed only on the apical surfaces of healthy epithelial cells (for instance, FRA⁸⁷, the urokinase receptor^{88,89} and certain mucins⁹⁰) may also provide unique opportunities for tumour-specific targeting. Specifically, receptors that are restricted to the apical surface of polarized epithelial cells (such as vascular epithelial cells) will be inaccessible to parenterally administered drugs owing to intercellular junctions (comprising adherens junctions, desmosomes, tight junctions and gap junctions), which prevent solutes and particles from crossing the epithelium⁹¹. However, upon malignant transformation, such apically restricted receptors frequently become accessible to intravenous drugs because intercellular junctions are lost during tumorigenesis and apically restricted receptors become randomly positioned over the entire cell surface (FIG. 3). Thus, a receptor that is normally present solely on the apical surface of an epithelial cell may still be a good receptor for tumour targeting if its expression persists in the non-polarized malignant cell. However, candidate receptors must remain tethered to the cell surface and not be cleaved or shed into circulation, as an accumulation of the receptor in the bloodstream will divert the ligand-targeted drug away from the tumour tissue^{92–95}.

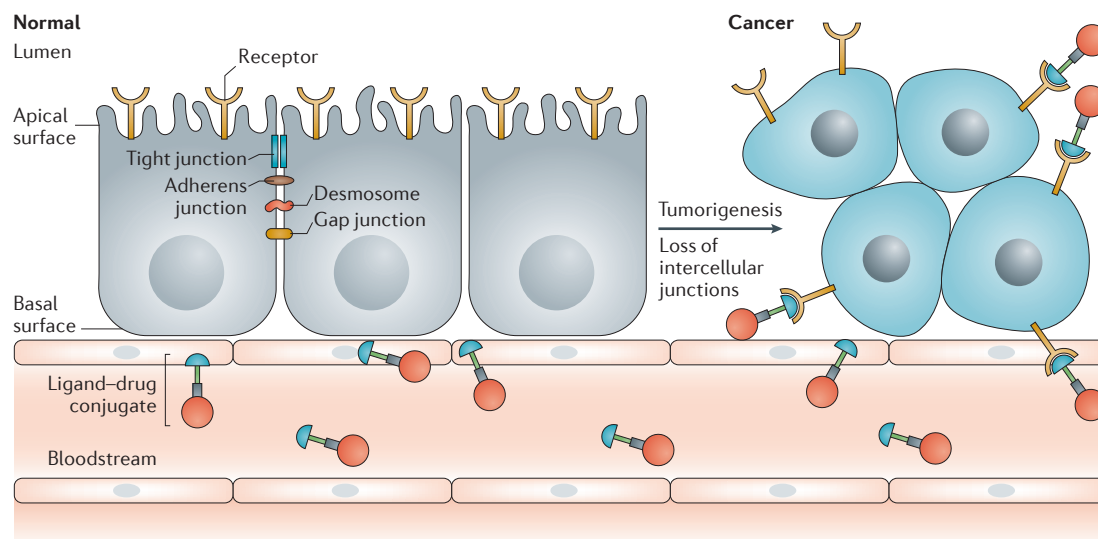


Figure 3 | The effect of epithelial-cell transformation on the accessibility of apical receptors. Owing to the loss of intercellular junctions (including tight junctions, adherens junctions, desmosomes and gap junctions) between epithelial cells upon malignant transformation, receptors that are normally located on the apical surface of a healthy epithelial cell (which are consequently normally inaccessible to parenterally administered drugs) become randomly distributed around the entire plasma membrane of a malignant cell, allowing easy access by targeted drugs.

Criteria for ligand selection

Once the ideal receptor for drug targeting is identified, a ligand with optimal affinity, specificity, size and functional-group availability must be designed for receptor-specific delivery. Criteria that govern the design and synthesis of such targeting ligands are described below.

Binding affinity. Given that the systemic dose of a ligand–drug conjugate required to saturate tumour-specific receptors will depend on the affinity of the ligand for its receptor, the higher the affinity of the ligand, the lower the concentration of drug necessary to achieve receptor saturation. Thus, a ligand–drug conjugate with nanomolar affinity will occupy all targeted receptors at a 1,000-fold lower concentration than will a ligand–drug conjugate with micromolar affinity, decreasing the chance of systemic toxicity from nonspecific deposition in healthy tissues. In our experience, only ligands with values of affinity for their receptors of dissociation constant (K_d) ~ 10 nM or lower should be pursued. Indeed, the successful targeting ligands that have been developed in our laboratory all bind to their cognate receptors with low nanomolar affinities^{82,96–98}. If ligands of sufficiently high affinity cannot be identified, then the ligation of multiple ligands to the same therapeutic payload can compensate with improved avidity^{99,100}. For example, the median lethal dose (LD_{50}) of a paclitaxel conjugate that targets HER2-expressing cancer cells with a peptide ligand was found to be 2.5 μ M, but this was improved to 160 nM simply by adding a second targeting peptide to the conjugate¹⁰¹.

Target selectivity. Tumour specificity will obviously be compromised if the targeting ligand recognizes other members of a receptor family that are not tumour-specific. For example, the SSTR family consists of five members,

of which only two are commonly upregulated in neuroendocrine cancers¹⁰² and therefore useful for tumour targeting. The use of a tumour-isoform-specific ligand will avoid toxicity to the healthy tissues that express a different isoform of the targeted receptor. Similarly, whereas gastrin (or cholecystokinin) receptor family members are widely distributed in healthy tissues, only a targeting ligand that is specific for CCKBR will be useful for tumour-specific targeting^{82,96}. If an isoform-specific ligand cannot be identified, ligands that bind to allosteric sites may be used, as allosteric binding sites generally differ more among family members than do orthosteric sites¹⁰³.

Derivatizability of ligand. The targeting ligand should preferably have a derivatizable functional group — such as a carboxylic acid, amine, alcohol, thiol or haloaromatic substituent — for facile conjugation to the desired imaging or therapeutic agent. These moieties enable rapid coupling to functional groups on the spacer via simple and robust chemistry (for instance, through the formation of amides, carbamates, oximes, esters, carbonates or disulphides^{97,104–107}). Unfortunately, in our experience, the attachment of such functional moieties can often interfere with the ability of a ligand to bind to its receptor. In this scenario, structure–activity relationships must be examined to identify sites on the ligand where modification will not interfere with receptor binding.

Size of ligand–drug conjugates. Although control over the size of the required therapeutic or imaging payload may be limited, there are often opportunities to adjust the size either of the targeting ligand or of the connecting linker to create a therapeutic conjugate with the desired pharmacokinetics^{78,108}. The fact that conjugate size can substantially influence the rate and magnitude of drug accumulation in solid tumours has been demonstrated

through the analysis of the kinetics of tumour uptake of a homologous series of folate–polyethylene-glycol (PEG)–rhodamine conjugates that consisted of folic acid tethered to rhodamine via PEG spacers of different molecular weights. Increasing the size of the PEG spacers in these conjugates was found to markedly reduce tumour penetration, and even small increases in PEG molecular weight could cause notable reductions in tumour accumulation¹⁰⁸. Clearly, if ligand size or linker size can be controlled without a substantial loss of receptor specificity or affinity, lower-molecular-weight components will generally be preferred.

In general, conjugate size can influence drug delivery into solid tumours via several important mechanisms. First, large drug carriers such as polymers and liposomes may passively accumulate in tumour tissues owing to the enhanced permeability and retention (EPR) effect, whereby defects or gaps in the tumour vasculature allow the extravasation and accumulation of larger particles (usually with diameters <600 nm)^{30,109} that would be retained within the blood vessels of healthy tissues. Unfortunately, further penetration of these same large particles is often hampered by the dense extracellular matrix that is found in most solid tumours (indeed, some tumour interiors can become anoxic because even oxygen diffusion is hindered) and by a malformed lymphatic system, leading to problems with the delivery of nanoparticles to cells deep within a tumour mass²⁹. However, such deficiencies in tumour penetration can be overcome if the low-molecular-weight therapeutic cargo can be released and allowed to diffuse independently into the tumour. This strategy has, in fact, been successfully used to deliver the entrapped doxorubicin from large, thermally sensitive liposomes into solid tumour tissue¹¹⁰. The impact of tumour biology on drug delivery has been reviewed elsewhere^{111–114}.

A second mechanism through which conjugate size can influence drug delivery relates to the effect of particle size on both the rate of excretion through the kidneys and the removal of the drug from the bloodstream by cells of the mononuclear phagocytic system (MPS). Particles or molecules that are smaller than ~40 kDa are typically extracted from the blood by the glomerulus into the urine and excreted from the body rapidly¹¹⁵, whereas particles larger than this threshold can circulate much longer within the vasculature¹¹⁶. Unfortunately, particles that are larger still — especially those that are >100 nm in diameter — are increasingly more aggressively scavenged from circulation by Kupffer cells and other phagocytic cells of the MPS. Thus, nanoparticles >100 nm in diameter may accumulate more prominently in the liver than in their intended pathologic tissues^{117,118}.

Although low-molecular-weight drug conjugates do not accumulate in solid tumours owing to the EPR effect, they will nevertheless passively perfuse a cancer mass more thoroughly and rapidly than do macromolecular drug carriers¹¹⁹. Moreover, any low-molecular-weight drug conjugate that is not captured by a receptor will generally be rapidly excreted from the body, reducing the likelihood of toxicity from unwanted drug release in

healthy tissues. In our experience, receptor saturation after intravenous administration of a low-molecular-weight drug conjugate is generally achieved 5–20 minutes following injection¹⁰⁸, and low-molecular-weight drug conjugates are commonly excreted with markedly faster kinetics than are larger conjugates. For example, etarfolatide (which has a relative molecular mass (M_r) of ~856), a folate-targeted imaging agent in Phase III clinical trials, is cleared primarily via urinary excretion with a half-life of 25 minutes¹²⁰, and the DNA-alkylating agent glufosamide (which has an M_r of ~383) is excreted with a half-life of 2.3 hours¹²¹. By contrast, the much larger PSMA-targeted liposomal nanomedicine BIND-014 (TABLE 1) exhibits a half-life in rats of more than 20 hours¹²². By minimizing the time a low-molecular-weight ligand-targeted therapeutic agent spends in circulation, the probability of premature drug release in healthy tissues, and thereby the likelihood of off-target toxicity, is reduced^{123,124}. However, the duration of drug conjugate exposure to receptor-expressing target tissues is also reduced.

Criteria for linker design

As the structural constraints on the design of the targeting ligand and therapeutic payload are often stringent, the optimization of the pharmacokinetic and pharmacodynamic properties of a targeted drug is generally achieved by modifying the linker chemistry. Moreover, injudicious linker design can compromise receptor affinity and/or payload efficacy, especially if the linker sterically interferes with ligand or payload function. Therefore, careful consideration of linker design is essential for optimal drug performance. The key elements of linker design are described below.

General physicochemical properties. Linkers or spacers that tether the targeting ligand to the therapeutic or imaging cargo can contribute to conjugate performance, as they can influence ligand–receptor binding and non-specific adsorption of the conjugate to off-target tissues, as well as affecting the pharmacokinetics and pharmacodynamics of tumour penetration, metabolism and excretion. If attachment of a desired drug in close proximity to the targeting ligand directly interferes with receptor binding, such steric obstruction can often be avoided by inserting an inobtrusive spacer between the ligand and its cargo. For example, PSMA-targeted imaging agents bind with much higher affinity when the ligand 2-[3-(1,3-dicarboxy propyl)-ureido]pentanedioic acid (DUPA) is connected to the imaging moiety via an alkyl chain that comprises at least six atoms¹²⁵. However, if such a spacer (for example, a short PEG) still compromises receptor binding, the avoidance of steric interference may require the selection of a more accessible site on the ligand for spacer attachment. Identification of preferred ligand attachment sites is often facilitated by structural information on the receptor–ligand complex, from which the regions of the receptor-bound ligand that are exposed to the aqueous medium can be identified and then used for linker attachment. For example, the structures of the naltrindole-bound μ -opioid and δ -opioid receptors show that an indole moiety on the

Table 1 | Ligand-targeted therapeutic agents in clinical development

Ligand-targeted drug (ligand–drug)	Target	Sponsor	Current stage of development and indication	ClinicalTrials.gov identifier	Refs
Vintafolide (folate–desacetylvinblastine hydrazide)	FR	Endocyte	Phase III in combination with liposomal doxorubicin (Doxil) for the treatment of platinum-resistant ovarian cancer*	NCT01170650	166
			Phase II in combination with docetaxel for NSCLC, ovarian and endometrial cancers	NCT01577654	206
EC0225 (folate–desacetylvinblastine-hydrazide or folate–mitomycin C)	FR	Endocyte	Phase I for solid tumours (refractory or metastatic)	NCT00441870	167
EC0489 (folate–desacetylvinblastine hydrazide with modified linker)	FR	Endocyte	Phase I for solid tumours (refractory or metastatic)	NCT00852189	135
EC1456 (folate–tubulysin)	FR	Endocyte	Phase I for solid tumours	NCT01999738	–
EC17 (folate–FITC–hapten)	FR	Endocyte	Phase II immunotherapy for renal cell carcinoma	NCT00485563	207
Epopolate (also known as BMS-753493; folic acid–epothilone)	FR	Bristol-Myers Squibb	Reached Phase II for advanced solid tumours, although development has since been halted	NCT0055017	168,169
Glufosamide (glucose–iphosphoramide)	GLUT1	Threshold Pharmaceuticals and Eleison Pharmaceuticals	Phase II for soft-tissue sarcomas (halted)	NCT00441467	175
			Phase III for metastatic pancreatic cancer as a second-line treatment	NCT01954992	174
NGR-TNF (Asn-Gly-Arg-TNF α)	APN	EORTC and MolMed S.p.A.	Phase II for soft tissue sarcomas	NCT00484341	176,177, 208
			Phase I for solid tumours	NCT00483093	
			Phase II for ovarian cancer	NCT01358071	
			Phase II for kidney cancer	NCT00484211	
			Cancers of the colorectal system (Phase II and pilot)	NCT00483080; NCT00675012	
GRN1005 (also known as ANG1005; angiopep 2–paclitaxel)	LRP1	AngioChem	Phase II for breast cancer with brain metastases	NCT01480583	8,178, 209
			Phase II in combination with trastuzumab for NSCLC with brain metastases	NCT01497665	
BIND-014 (PSMA-targeted liposomal docetaxel)	PSMA	Bind Therapeutics	Phase II for prostate cancer	NCT01812746	186
			Phase II for NSCLC	NCT01792479	
			Phase II for solid tumours	NCT01300533	

APN, aminopeptidase N; EORTC, European Organization for Research and Treatment of Cancer; FITC, fluorescein isothiocyanate; FR, folate receptor; GLUT1, glucose transporter 1; LRP1, low-density lipoprotein receptor-related protein 1; NSCLC, non-small-cell lung cancer; PSMA, prostate-specific membrane antigen; TNF α , tumour necrosis factor- α . *Enrolment in this trial was suspended in May 2014 following a recommendation from the data safety and monitoring board, based on lack of efficacy. No safety concerns were identified. The data are currently being reviewed.

antagonist protrudes from the binding cleft and is accessible to the surrounding solution¹²⁶. Clearly, the conjugation of the linker to the antagonist at this site should reduce any loss in antagonist affinity.

In some cases, decreases in ligand-binding affinity can also result from unwanted intramolecular associations between the ligand and its tethered cargo. If this occurs, a more rigid spacer can prevent such intramolecular interference¹²⁷. For example, Ueda and colleagues¹²⁸ found that a rigid spacer (namely, triazolyl-phenyl) markedly enhanced the affinity of jasmonate for its receptor compared with a similar construct that lacked the spacer. With a fully optimized spacer, the affinity

of the ligand–drug conjugate for the targeted receptor should be similar to the affinity of the free ligand for the same receptor.

Targeting ligands and chemotherapeutic agents are often designed to be hydrophobic to maximize membrane permeability and receptor affinity. As such hydrophobicity may promote unwanted nonspecific associations with lipoproteins, scavenger receptors and lipid bilayers or membranes, it may be useful to use a linker that will confer overall hydrophilicity¹²⁹ on the final ligand–drug conjugate. These spacers can be made of polysaccharide¹³⁰, hydrophilic amino acids, PEGs of varying lengths or peptidoglycans^{131,132}. Such

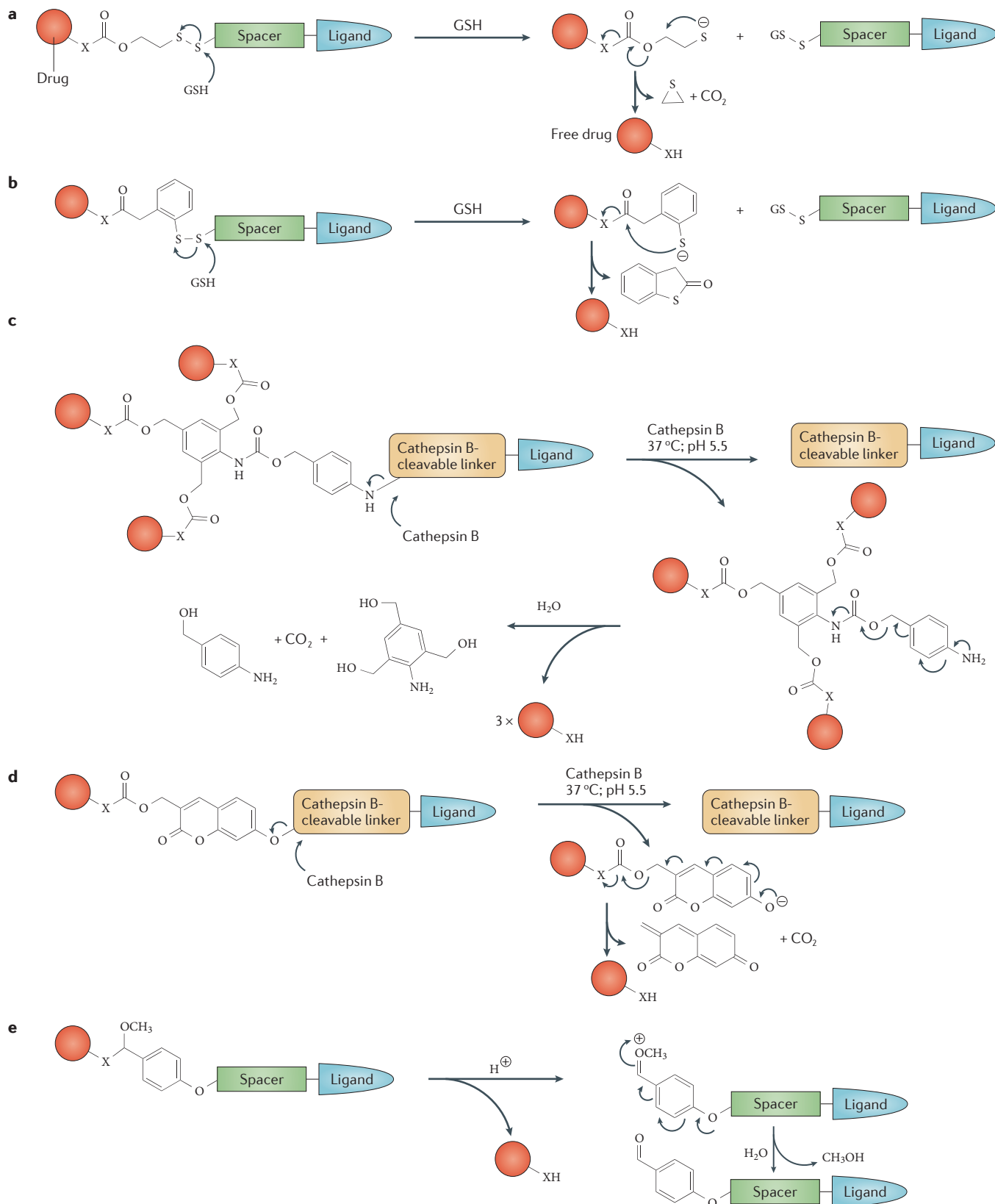


Figure 4 | **Common strategies for intracellular drug release using self-cleaving linkers.** **a,b** | The reduction of a disulphide bond by excess intracellular glutathione (GSH) triggers the release of the unmodified drug^{131,143}. **c,d** | Lysosomal cathepsin B initiates the release of the drug by cleaving a peptide linker (in this case,

a valine–citrulline bond)¹⁴⁵. **e** | The high concentration of protons within some endosomal compartments (for instance, inside lysosomes) can be exploited to promote the release of a drug by inducing the cleavage of a high-pH-sensitive bridge — for example, an acetal linker (that is, X=O)¹³¹.

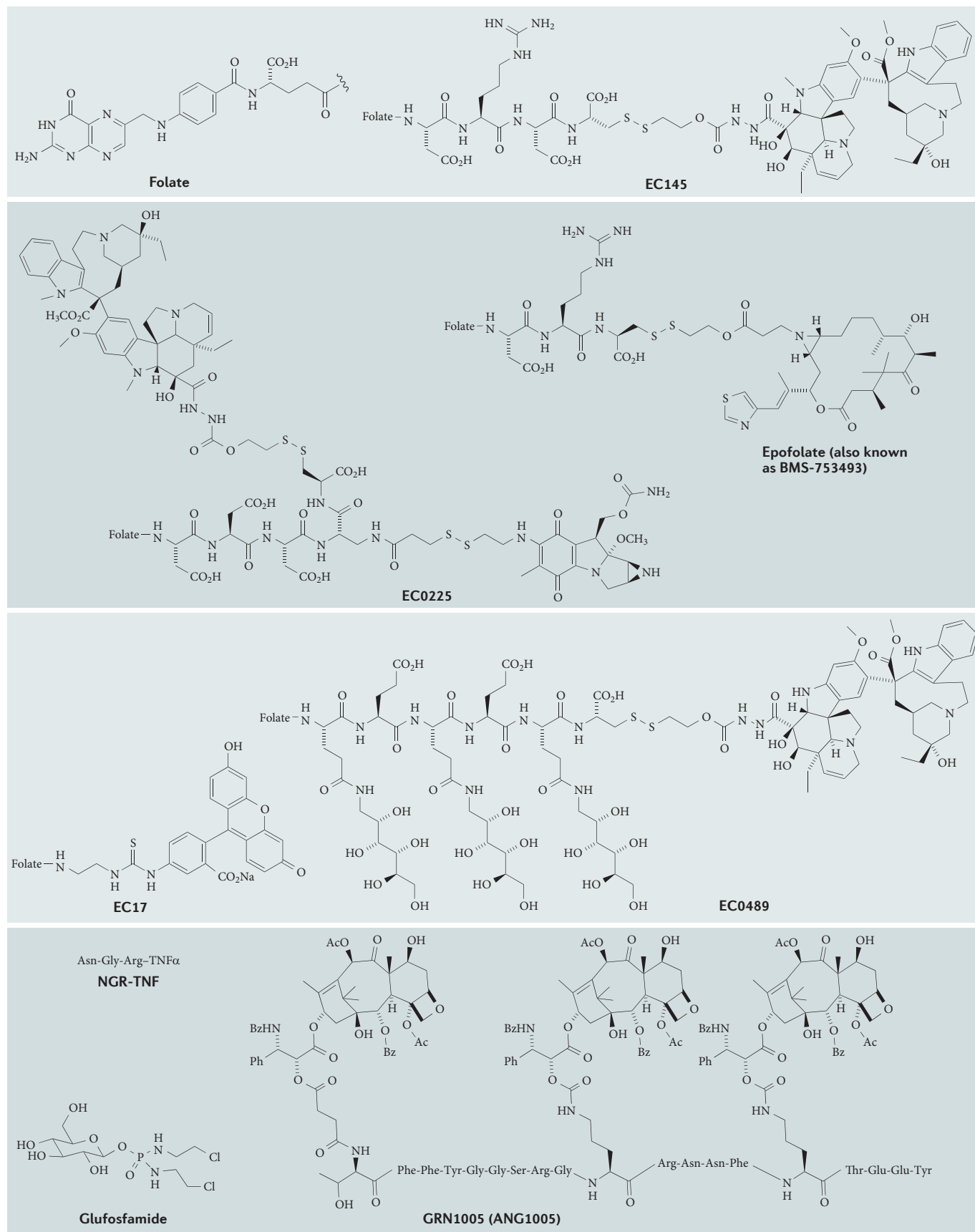


Figure 5 | Structures of ligand-targeted therapeutic agents that are currently undergoing clinical trials. The structure of folate, which is

used to target several agents included here to tumour folate receptors, is shown in the top left. TNF α , tumour necrosis factor- α .

water-soluble spacers may not only reduce nonspecific interactions but also prevent the passive penetration of the cytotoxic conjugate into receptor-negative cells¹³³.

The rate and route of tumour penetration and conjugate excretion can also be strongly influenced by judicious selection of the spacer chemistry. In general, we prefer that any ligand–drug conjugates that are not captured by their targeted receptors be rapidly excreted by the kidneys, as prolonged circulation can lead to premature drug release and the associated off-site toxicity. To achieve rapid kidney excretion, we again desire our conjugates to be hydrophilic¹³⁴, as reduced plasma-protein binding and limited nonspecific adsorption can facilitate kidney filtration. Moreover, as highly anionic conjugates are often cleared by organic anion transporters in the liver, the use of multiple negatively charged groups in the linker can bias the extent of excretion from the kidneys towards the liver, bile duct and gut, leading to slower excretion from the body and a higher probability of off-target drug release¹³⁵. Furthermore, the presence of peptide-scavenger receptors in the liver and kidneys can promote unwanted retention of peptide-containing spacers by both systems¹³⁶. For example, in a Phase I clinical trial of vintafolide, constipation resulting from hepatic–biliary clearance of the drug was identified as the dose-limiting toxicity. To reduce this hepatic–biliary deposition of the drug in the gut, the tetrapeptide spacer was replaced with a more hydrophilic glucitoyl- γ -glutamate spacer, resulting in predominantly renal clearance. The use of the re-engineered spacer alleviated the constipation and enabled the unbound drug to be excreted via a less toxic route¹³⁵.

Use of cleavable bridges. Whereas a non-cleavable bridge between a ligand and an attached imaging agent is generally preferred, a cleavable bridge is usually desired for delivery of therapeutic cargoes, as the release of the unmodified cytotoxic agent is often required for maximal drug efficacy⁷⁷ (FIG. 4). Such cleavable linkers must remain intact during transit through the vasculature to the tumour but must lyse rapidly upon capture and internalization by the malignant cell¹³⁷. As receptor-mediated endocytosis constitutes a major pathway of ligand-targeted drug delivery, the use of self-cleaving linkers, such as acetals (FIG. 4e), hydrazones^{57,138} and esters that are hydrolysed at the acidic pH found in many endosomes¹³⁷, has become a popular strategy for intracellular drug release. Other chemistries that lend themselves to intracellular drug release include disulphide reduction¹³⁹ (FIG. 4a,b) and endosomal enzyme hydrolysis^{140–142} (FIG. 4c,d). In most cases, an elimination cascade should be designed into the linker to ensure that no atoms from the spacer remain attached to the released drug. Several such self-cleaving release chemistries have been described in the literature^{143–145}.

Criteria for payload selection

An optimally designed linker and targeting ligand will be of little value if the therapeutic payload is unable to kill the cancer cell. However, cytotoxicity depends on the intrinsic toxicity of the therapeutic agent, the efficiency of the release of the therapeutic payload from the targeting

ligand–linker complex, the avoidance of multidrug efflux pumps and intracellular metabolism, and the ability of the therapeutic agent to reach its intended intracellular target. Unfortunately, not all therapeutic payloads meet all of these criteria, so careful selection of an appropriate therapeutic agent is essential for eventual clinical success.

Drug potency. As most ligand–drug conjugates are designed to deliver only one therapeutic molecule per ligand, the potency of the attached drug must be high in order to achieve maximal killing of cancer cells. In the case of folate-targeted drugs, as receptor numbers may exceed 10^6 per cancer cell, an IC_{50} of $<10^{-8}$ M has generally been found to be sufficient, as long as the affinity of the ligand has not been compromised by attaching the drug molecule. If the number of available receptors is below 10^6 per cell⁵⁰, drugs of even greater potency will be required. Although it is tempting to propose that such limitations on potency can be solved simply by attaching more therapeutic warheads to the same targeting ligand, it is generally much easier to develop a single drug molecule with a tenfold higher potency than it is to attach ten molecules of the same lower-potency drug. Indeed, with the exception of GRN1005 (REF. 144), all of the ligand-targeted drug conjugates currently in clinical trials are linked to high-potency drugs that have low-nanomolar or subnanomolar IC_{50} values³ (TABLE 1; FIG. 5).

Mechanism of action. In our opinion, chemotherapeutics that block fundamental processes associated with cell proliferation and survival — such as cytokinesis, DNA replication, anti-apoptotic processes or protein synthesis — may prove more ‘resistance-proof’ than might agents that interrupt upstream signalling pathways, because such blockades can often be bypassed by the activation of a downstream effector in the same or a parallel pathway^{146,147}. It is also important to recognize that if tumour targeting is sufficiently specific, toxic agents that disrupt essential metabolic processes that are not unique to the transformed state (for example, glycolysis^{148,149}, glutaminolysis¹⁵⁰, (Na⁺, K⁺)-ATPase function^{151,152} and sugar transport¹⁴⁹) or that activate fundamental mechanisms of apoptosis might also prove effective as targeted chemotherapeutic agents^{153–155}. Resistance mechanisms that can evade targeted inhibition of these fundamental processes may be slow to develop, as few alternative mechanisms exist.

Drug release and metabolism within the targeted cell.

Even with the inclusion of a self-cleaving linker that enables an unmodified drug to be released following receptor-mediated endocytosis, the released drug must still escape the encapsulating endosome to be therapeutically active. Most well-established chemotherapeutic agents already exhibit adequate membrane permeability, as they have demonstrated potency when added to intact cells. By contrast, peptides, oligonucleotides, antibodies and proteins do not generally diffuse passively across lipid bilayers and therefore become trapped within the endosomes until they are released by some exogenous mechanism. Cell-permeating

Self-cleaving linkers

Tethers between targeting ligands and the imaging or therapeutic cargo that cleave upon (but not before) internalization of the conjugate inside tumour cells.

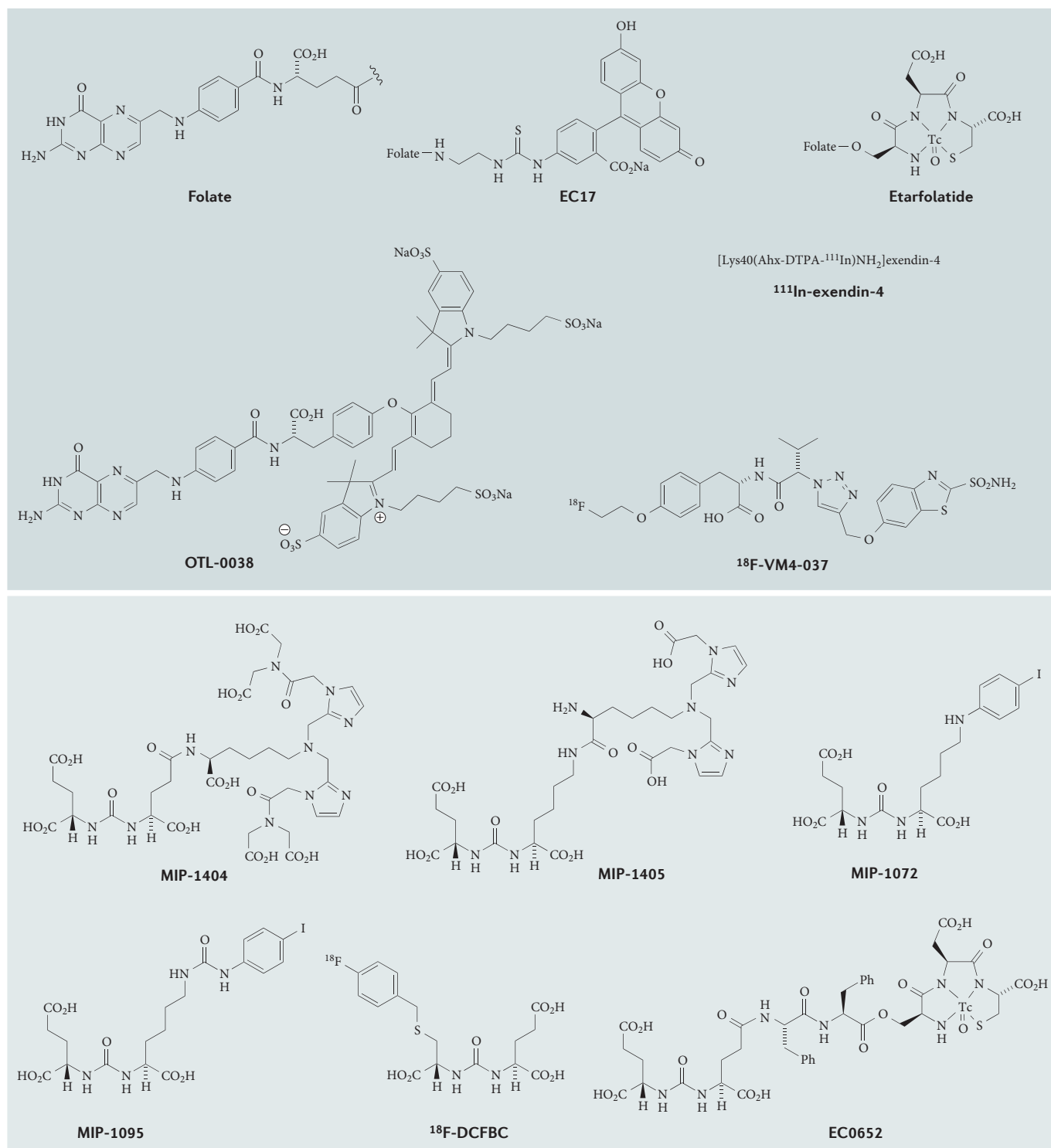


Figure 6 | Structures of ligand-targeted imaging agents that are currently undergoing clinical trials. The structure of folate, which targets several imaging agents included here to tumour folate receptors, is shown in the top left.

peptides^{156,157}, pore-forming and caged fusogenic or cationic lipids^{156,158–160}, and photothermally activated complexes¹⁶¹ have all been investigated for use in promoting drug egress from endosomes¹⁶². However, in each of these cases, notable heterogeneity and bulk have been

added to the intended drug product, rendering the path to regulatory approval more difficult. Clearly, further improvements in facilitating drug escape from the endosome will be required before the intracellular delivery of biologic therapeutics can reach its full potential.

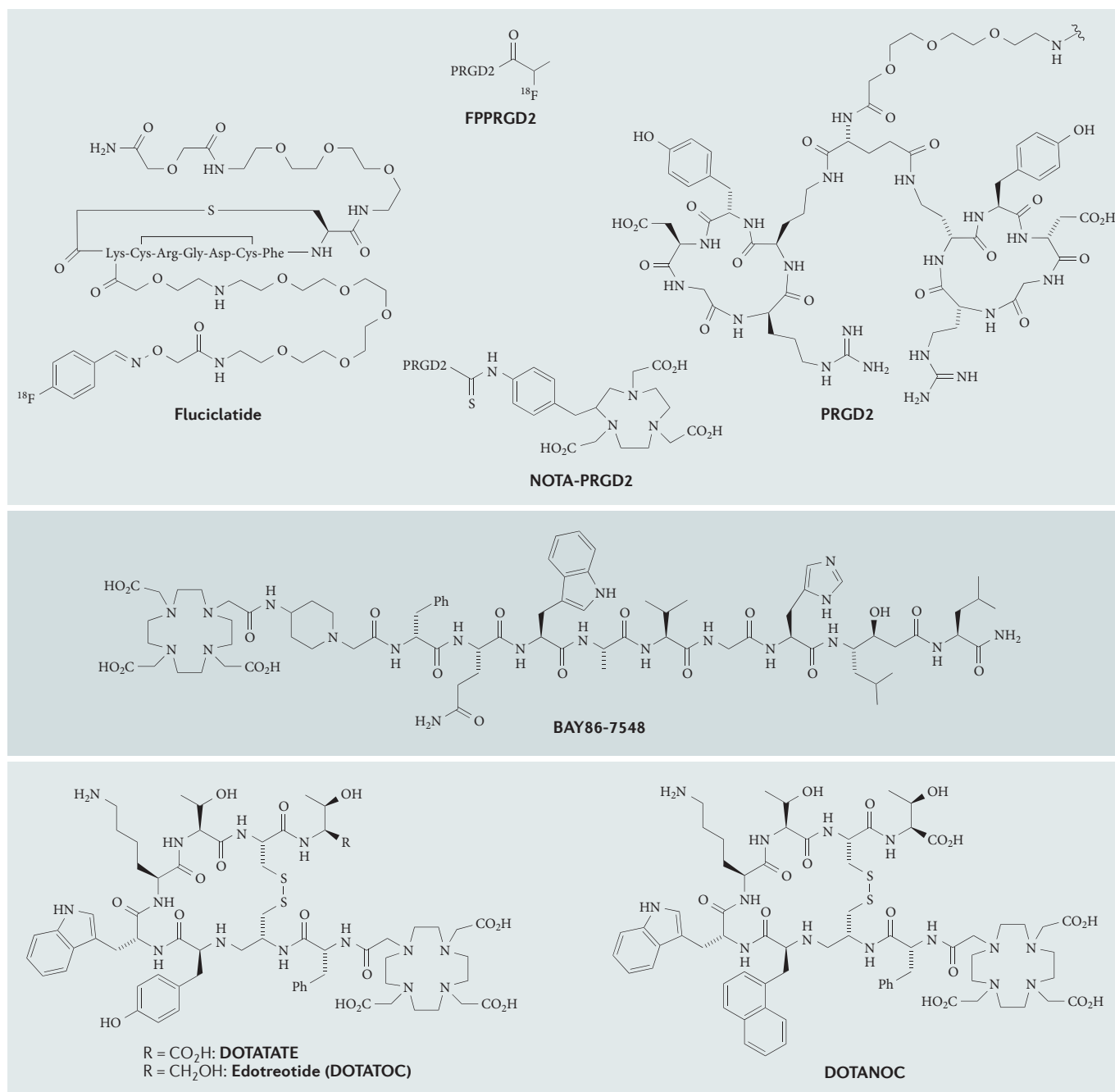


Figure 7 | **Additional structures of ligand-targeted imaging agents that are currently undergoing clinical trials.**

PRGD2 (PEGylated arginine-glycine-aspartic acid dimer), which features in several of the structures featured here, is shown in the top right. DOTATATE, tetraazacyclododecane tetraacetic acid-octreotide; DOTATOC, DOTA-(tyrosine 3)-octreotide; DUPA, 2-[3-(1,3-dicarboxypropyl)-ureido]pentanedioic acid.

Ligand-targeted therapeutics in trials

As mentioned above, FRa is overexpressed on many epithelial cancers, including cancers of the ovary¹⁶³, breast⁸⁷, lung¹⁶⁴, kidney⁵⁰ and colon¹⁶⁵. As the chemistry for the conjugation of folate to therapeutic and imaging agents is well characterized¹², folate-linked drugs currently constitute a large proportion of ligand-targeted drugs in clinical trials (FIG. 5; TABLE 1). Encouragingly, a recent interim analysis of Phase II data comparing

vintafolide plus docetaxel with docetaxel alone showed promise of the combination treatment for extending overall survival of individuals with non-small-cell lung cancer (NSCLC)¹⁶⁶. Most notably, the Phase IIb trial data (ClinicalTrials.gov identifier: NCT01577654) indicate that the combination therapy improves median progression-free survival from 3.0 months to 4.2 months, with an increased median overall survival of 5.9 months (from 6.6 months to 12.5 months).

EC0225, a folate conjugate that comprises two separate therapeutic warheads, and EC0489, a folate–vincalalkaloid conjugate similar to vintafolide but containing a linker that reduces biliary clearance, are both undergoing Phase I evaluation for the treatment of refractory solid or metastatic tumours (NCT00441870 and NCT00852189, respectively)¹⁶⁷. Epopolate (BMS-753493), a folic acid–epothilone conjugate, completed Phase I and Phase II assessments for the treatment of advanced solid tumours but, owing to lack of efficacy, has been withdrawn from further clinical investigation^{168,169}. A considerably more potent folate–tubulysin conjugate, EC1456, entered clinical trials this year (NCT01999738), and EC0905, a folate–vinblastine conjugate, has shown considerable promise in preclinical studies for treating spontaneous bladder cancers in dogs¹⁷⁰.

Several glucose-linked drugs designed to deliver attached therapeutics to tumours that overexpress a glucose transporter are also undergoing clinical evaluation or late preclinical development^{171–173}. Most notably, glufosfamide — a glucose conjugate of iphosphoramidate — has advanced to Phase III clinical trials (NCT01954992)¹⁷⁴, in which it is being assessed for treatment of metastatic pancreatic cancer. Glufosfamide has also proved effective against soft-tissue sarcomas, for which it progressed into Phase II trials (NCT00441467)^{174,175}; however, its development for this indication seems to have been halted. The NGR (Asn-Gly-Arg) peptide ligand which targets aminopeptidase N (a cell surface receptor that is overexpressed in many cancers), is also undergoing evaluation as a conjugate with tumour necrosis factor- α for treatment of solid tumours (NCT00483093)^{176,177}. Low-density lipoprotein receptor-related protein 1 (LRP1), a cell surface receptor that is involved in cancer metastasis, has been successfully targeted by a small-molecule drug conjugate that consists of three molecules of paclitaxel linked to the homing peptide, angioprep 2 (REF. 8). This conjugate, named GRN1005, is currently undergoing Phase II trials for the treatment of NSCLC with brain metastases (NCT01497665). In addition, GRN1005 in combination with trastuzumab has advanced to Phase II studies as a therapeutic agent for breast cancer (NCT01480583)¹⁷⁸.

Ligand-targeted imaging agents

Ligand-targeted cancer-imaging agents are also demonstrating success in clinical trials by identifying and localizing tumour masses, and by selecting patients for corresponding ligand-targeted treatment (FIGS 6.7; TABLE 2). For example, the folate-targeted radioimaging agent etarfolatide has not only established its utility for imaging FR-positive malignant disease in individuals with lung, kidney, brain or ovarian cancer but also proved useful in identifying metastases in the lymph nodes of patients with lung cancer¹⁷⁹. Moreover, etarfolatide has proved useful in selecting the patients with ovarian or lung cancer who subsequently display a greater probability of responding to a folate-targeted therapy than do non-selected patients¹⁸⁰.

Folate-targeted fluorescent dyes have also proved beneficial as tools to aid surgeons in the identification of malignant disease during surgery. For example, data from

a trial of ten individuals with ovarian cancer found that fivefold as many malignant lesions could be removed with the aid of the folate-targeted fluorescent dye than with standard visual and tactile methods¹⁸¹. More importantly, all of the resected fluorescent lesions in this trial were subsequently confirmed by pathology to be malignant.

Ligands that can deliver attached imaging agents selectively to PSMA overexpressed in prostate cancers have shown effectiveness in clinical trials (FIGS 6.7; TABLE 2). EC0652, a ^{99m}Tc-conjugate of the PSMA-targeting ligand DUPA^{98,125}, and several related PSMA-targeting positron emission tomography (PET)-imaging agents have each demonstrated high specificity for prostate cancer metastases in Phase 0, Phase I and/or Phase II clinical trials^{182–185} (FIGS 6.7; TABLE 2). In addition to these imaging agents, a PSMA-targeted nanoparticle formulation of docetaxel is in clinical development¹⁸⁶, with one DUPA–tubulysin conjugate, EC1169 (REF. 187), in Phase I trials (NCT02202447), and a second, EC1719, that will soon enter Phase I trials.

Other ligand-targeted radioimaging agents in human clinical trials include somatostatin analogues that are linked to radionuclide-chelating agents, such as edotreotide (DOTATOC), DOTATATE (tetraazacyclododecane tetraacetic acid-octreotate; NCT01873248 and NCT01967537) and DOTANOC (DOTA-(tyrosine 3)-octreotide; NCT01747096) (FIGS 6.7; TABLE 2), which are being used to image neuroendocrine tumours^{188–191}. SSTR2-targeted radiotherapeutics that use lutetium-177 and yttrium-90 are also currently under evaluation^{192,193}. Other notable targeted imaging agents in clinical trials include: ¹¹¹In-exendin-4, which targets glucagon-like peptide 1 receptor and is being tested for imaging insulinomas (NCT02127541 and NCT00937079)¹⁹⁴; NOTA (1,4,7-triazacyclononane-1,4,7-triacetic acid)-(PEGylated arginine-glycine-aspartic acid dimer) PRGD2 and fluciclatide, which target $\alpha_v\beta_3$ integrin and are being tested in lung cancer (NCT01527058)^{195–200}; ¹⁸F-VM4-037, an imaging agent that has completed Phase II trials in kidney cancer (NCT01712685) and targets carbonic anhydrase 9, which is overexpressed in hypoxic tumours; and BAY86-7548, a ⁶⁸Ga-imaging agent that has been evaluated in prostate cancer (NCT01205321) and that targets the bombesin receptor subtype 2 (REF. 201) (FIGS 6.7; TABLE 2).

Conclusions

Low-molecular-weight ligand-targeted drugs have several advantages over traditional non-targeted therapeutic agents. First, targeted drugs will generally reduce unwanted toxicities by delivering the therapeutic warheads specifically to pathologic cells, thereby reducing the exposure of healthy cells to the drug. Second, patients that overexpress the targeted receptor in their diseased tissues can generally be identified before therapy by imaging the patient using the same targeting ligand linked to a radiotracer. Companion diagnostics of this sort not only minimize the number of patients who might fail to benefit from the therapy but may also improve the safety and efficacy of the corresponding therapeutic, increasing the likelihood of regulatory approval.

Table 2 | Ligand-targeted cancer imaging agents in clinical trials*

Ligand-targeted imaging agent (ligand-imaging-agent)	Target	Sponsor	Current stage of development	ClinicalTrials.gov identifier	Refs
EC17 (folate-fluorescein)	FR	On Target Laboratories	Phase II study of fluorescence-guided surgery of ovarian cancer	NCT01511055	207
OTL-0038 (Pte-Tyr-NIR-dye)	FR	On Target Laboratories	Phase II study of fluorescence-guided surgery of ovarian, breast, lung and kidney cancers	NCT02317705	210
Etarfolatide (folate- ^{99m} Tc)	FR	Endocyte	Phase III trials in FR-positive cancer	NCT01577654; NCT01170650; NCT01394679	179
Fluciclatide (Arg-Gly-Asp-PEGylated ¹⁸ F-PET or ¹⁸ F-CT agent)	$\alpha_v\beta_3$ integrin	GE Healthcare	Phase II response evaluation in kidney cancer	NCT01961583	195–197
			Phase II response evaluation in brain, colon, head and neck, and lung cancers	NCT00565721	
			Phase II response evaluation of several drugs for angiogenesis	NCT00117650	
NOTA-PRGD2 (Arg-Gly-Asp-NOTA- ¹⁸ F, Arg-Gly-Asp-NOTA- ^{99m} Tc or Arg-Gly-Asp-NOTA- ⁶⁸ Ga)	$\alpha_v\beta_3$ integrin	Peking Union Medical College Hospital	Phase 0 study in lung cancer (⁶⁸ Ga)	NCT01527058	198–200
			Phase 0 study in glioma (⁶⁸ Ga)	NCT01801371	
¹²³ I-MIP-1072 and ¹²³ I-MIP-1095 (Glu-heterodimer- ¹²³ I)	PSMA	Molecular Insight Pharmaceuticals	Phase I imaging of prostate cancer (alone, and in comparison with the ¹¹¹ In-mono-clonal antibody ProstaScint scan)	NCT00712829	211
^{99m} Tc-MIP-1404 and ^{99m} Tc-MIP-1405 (Glu-heterodimer- ^{99m} Tc)	PSMA	Molecular Insight Pharmaceuticals	Phase II diagnostic imaging of prostate cancer	NCT01667536; NCT01667536	212
EC0652 (DUPA- ^{99m} Tc)	PSMA	Purdue University	Phase 0–II imaging of prostate cancer	Not yet available	98,125
¹⁸ F-DCFBC (Glu-carbamoyl-Cys- ¹⁸ F)	PSMA	Sidney Kimmel Comprehensive Cancer Center	Phase II detection and imaging of metastatic prostate cancer	NCT01815515	185
DOTATATE (Oct-DOTA- ⁶⁸ Ga)	SSTR2	Multiple sponsors	Phase II imaging of neuroendocrine tumours	NCT01873248; NCT01967537	188–191
Edotreotide (also known as DOTATOC; Phe-Tyr-Oct-DOTA)	SSTR2	NCI	Phase III in malignant glioma	NCT01460706	212
			Phase I in other brain and carcinoid tumours	NCT02194452	
DOTANOC (Tyr-Nal ^c -Oct-DOTA- ⁶⁸ Ga)	SSTR2	Multiple sponsors	Phase III in gastroenteropancreatic neuroendocrine tumours	NCT01747096	189,190
¹¹¹ In-exendin-4 (exendin-4-DTPA- ¹¹¹ In)	GLP1R	University Hospital, Basel	Phase II/III imaging of insulinomas and transplanted islet cells	NCT02127541; NCT00937079	194
¹⁸ F-VM4-037 (CA9-targeting sulphonamide)	CA9	Siemens Molecular Imaging	Phase II in kidney tumours	NCT01712685	–
			Phase 0 in lung, head and neck, kidney and liver cancers	NCT00884520	
BAY86-7548 (bombesin- ⁶⁸ Ga)	BR subtype 2	Piramal Imaging SA	Phase I imaging of prostate tumours	NCT01205321	201

$\alpha_v\beta_3$ integrin, vitronectin receptor; BR, bombesin receptor; CA9, carbonic anhydrase IX; CT, computed tomography; DOTA, 1,4,7,10-tetraazacyclododecane-1,4,7,10-tetraacetic acid; DOTATATE, tetraazacyclododecane tetraacetic acid-octreotate; DOTATOC, DOTA-(tyrosine 3)-octreotide; DUPA, 2-[3-(1,3-dicarboxypropyl)ureido]pentanedioic acid; DTPA, diethylene triamine pentaacetic acid; FR, folate receptor; GLP1R, glucagon-like protein receptor 1; Nal, naphthyl side chain; NCI, US National Cancer Institute; NIR, near-infrared; NOTA, 1,4,7-triazacyclononane-1,4,7-triacetic acid; Oct, octreotide; PRGD2, PEGylated arginine-glycine-aspartic acid dimer; PET, positron-emission tomography; PSMA, prostate-specific membrane antigen; Pte-Tyr, pteroyl-tyrosine; SSTR2, somatostatin receptor 2. *Listed imaging agents include only those currently recorded on the ClinicalTrials.gov website (clinical trials approved by the US Food and Drug Administration).

Third, ligand-targeted therapeutics also offer greater flexibility for drug optimization than do standard non-targeted therapeutics, primarily because drug safety and drug efficacy are engineered into structurally distinct and independently variable parts of the molecule. For instance, if adequate drug efficacy is not achieved with

an initial drug payload, the therapeutic warhead can be repeatedly substituted until the optimal conjugate is identified. Similarly, drug safety is compromised by toxic side effects that result from the targeting of a given drug to healthy cells or organs; the targeting ligand can be independently exchanged until adequate

tumour specificity is achieved. As noted above, linker chemistries can also be optimized until the desired pharmacokinetics and pharmacodynamics are similarly obtained²⁰².

Finally, ‘well-behaved’ tumour-targeting ligands can be exploited for additional applications beyond the immediate objective of treating the right patient with the right drug, including the facilitation of optimal tumour resection during surgery with ligand-targeted near-infrared dyes and the isolation of circulating tumour cells from patient blood samples with immobilized

tumour-specific ligands¹⁸¹. The implementation of these applications has been facilitated by the use of much brighter and/or tissue-transparent tumour-targeted dyes^{96,203} that allow not only the visualization of more-deeply buried malignant lesions during surgery but also — with the aid of multiphoton intravital microscopy — the quantification of circulating tumour cells *in vivo*^{204,205}. Additional applications of tumour-specific ligands are emerging; with multiple ligand-targeted drugs in clinical trials, the future of the field seems promising.

1. Allen, T. M. Ligand-targeted therapeutics in anticancer therapy. *Nature Rev. Cancer* **2**, 750–763 (2002).
2. van der Meel, R., Vehmeijer, L. J., Kok, R. J., Storm, G. & van Gaal, E. V. Ligand-targeted particulate nanomedicines undergoing clinical evaluation: current status. *Adv. Drug Deliv. Rev.* **65**, 1284–1298 (2013).
3. Chari, R. V. J., Miller, M. L. & Widdison, W. C. Antibody–drug conjugates: an emerging concept in cancer therapy. *Angew. Chem. Int. Ed.* **53**, 3796–3827 (2014).
4. Wang, A. Z. & Farokhzad, O. C. Current progress of aptamer-based molecular imaging. *J. Nucl. Med.* **55**, 353–356 (2014).
5. Zhang, X. *et al.* A cell-based single-stranded DNA aptamer specifically targets gastric cancer. *Int. J. Biochem. Cell Biol.* **46**, 1–8 (2013).
6. Yu, B., Tai, H. C., Xue, W., Lee, L. J. & Lee, R. J. Receptor-targeted nanocarriers for therapeutic delivery to cancer. *Mol. Membr. Biol.* **27**, 286–298 (2010).
7. Shahied, L. S. *et al.* Bispecific minibodies targeting HER2/neu and CD16 exhibit improved tumor lysis when placed in a divalent tumor antigen binding format. *J. Biol. Chem.* **279**, 53907–53914 (2004).
8. Kurzrock, R. *et al.* Safety, pharmacokinetics, and activity of GRN1005, a novel conjugate of angiopep-2, a peptide facilitating brain penetration, and paclitaxel, in patients with advanced solid tumors. *Mol. Cancer Ther.* **11**, 308–316 (2012).
9. Zhang, X. X., Eden, H. S. & Chen, X. Peptides in cancer nanomedicine: drug carriers, targeting ligands and protease substrates. *J. Control Release* **159**, 2–13 (2012).
10. Rana, S. *et al.* Screening of a novel peptide targeting the proteoglycan-like region of human carbonic anhydrase IX. *Mol. Imag.* **12**, 497–509 (2013).
11. McGuire, M. J. *et al.* Identification and characterization of a suite of tumor targeting peptides for non-small cell lung cancer. *Sci. Rep.* **4**, 4480 (2014).
12. Xia, W. & Low, P. S. Folate-targeted therapies for cancer. *J. Med. Chem.* **53**, 6811–6824 (2010).
13. Varghese, B. *et al.* Folate receptor- β in activated macrophages: ligand binding and receptor recycling kinetics. *Mol. Pharm.* **11**, 3609–3616 (2014).
14. Vaitilingam, B. *et al.* A folate receptor- α -specific ligand that targets cancer tissue and not sites of inflammation. *J. Nuclear Med.* **53**, 1127–1134 (2012).
15. Thomas, M. *et al.* Ligand-targeted delivery of small interfering RNAs to malignant cells and tissues. *Ann. NY Acad. Sci.* **1175**, 32–39 (2009).
16. Shen, J., Chelvam, V., Cresswell, G. & Low, P. S. Use of folate-conjugated imaging agents to target alternatively activated macrophages in a murine model of asthma. *Mol. Pharm.* **10**, 1918–1927 (2013).
17. Sassoon, I. & Blanc, V. Antibody–drug conjugate (ADC) clinical pipeline: a review. *Methods Mol. Biol.* **1045**, 1–27 (2013).
18. Ducry, L. *Antibody–Drug Conjugates*. (Humana Press, 2013).
19. Bander, N. H. Antibody–drug conjugate target selection: critical factors. *Methods Mol. Biol.* **1045**, 29–40 (2013).
20. Haddley, K. Trastuzumab emtansine for the treatment of HER2-positive metastatic breast cancer. *Drugs Today* **49**, 701–715 (2013).
21. Perini, G. F. & Pro, B. Brentuximab vedotin in CD30+ lymphomas. *Biol. Ther.* **3**, 15–23 (2013).
22. Trapani, G., Denora, N., Trapani, A. & Laquintana, V. Recent advances in ligand targeted therapy. *J. Drug Target.* **20**, 1–22 (2012).
23. Liu, X. *et al.* Enhanced immune response induced by a potential influenza A vaccine based on branched M2e polypeptides linked to tuftsin. *Vaccine* **30**, 6527–6533 (2012).
24. Jeannin, P. *et al.* Immunogenicity and antigenicity of synthetic peptides derived from the mite allergen Der p 1. *Mol. Immunol.* **30**, 1511–1518 (1993).
25. Adem, Y. T. *et al.* Auristatin antibody drug conjugate physical instability and the role of drug payload. *Bioconjug. Chem.* **25**, 656–664 (2014).
26. Zimmerman, E. S. *et al.* Production of site-specific antibody–drug conjugates using optimized non-natural amino acids in a cell-free expression system. *Bioconjug. Chem.* **25**, 351–361 (2014).
27. Behrens, C. R. & Liu, B. Methods for site-specific drug conjugation to antibodies. *MAbs* **6**, 46–53 (2014).
28. Firer, M. A. & Gellerman, G. Targeted drug delivery for cancer therapy: the other side of antibodies. *J. Hematol. Oncol.* **5**, 1756–8722 (2012).
29. Jain, R. K. & Stylianopoulos, T. Delivering nanomedicine to solid tumors. *Nature Rev. Clin. Oncol.* **7**, 653–664 (2010).
30. Yuan, F. *et al.* Vascular permeability in a human tumor xenograft: molecular size dependence and cutoff size. *Cancer Res.* **55**, 3752–3756 (1995).
31. Weinstein, J. N. & van Osdol, W. Early intervention in cancer using monoclonal antibodies and other biological ligands: micropharmacology and the “binding site barrier”. *Cancer Res.* **52**, 2747s–2751s (1992).
32. van Osdol, W., Fujimori, K. & Weinstein, J. N. An analysis of monoclonal antibody distribution in microscopic tumor nodules: consequences of a “binding site barrier”. *Cancer Res.* **51**, 4776–4784 (1991).
33. Lee, H., Fonge, H., Hoang, B., Reilly, R. M. & Allen, C. The effects of particle size and molecular targeting on the intratumoral and subcellular distribution of polymeric nanoparticles. *Mol. Pharm.* **7**, 1195–1208 (2010).
34. Kostarelou, K. *et al.* Binding and interstitial penetration of liposomes within avascular tumor spheroids. *Int. J. Cancer* **112**, 713–721 (2004).
35. Juweid, M. *et al.* Micropharmacology of monoclonal antibodies in solid tumors: direct experimental evidence for a binding site barrier. *Cancer Res.* **52**, 5144–5153 (1992).
36. Shin, G. *et al.* GENT: gene expression database of normal and tumor tissues. *Cancer Informat.* **10**, 149–157 (2011).
37. Rhodes, D. *et al.* ONCOMINE: a cancer microarray database and integrated data-mining platform. *Neoplasia* **6**, 1–6 (2004).
38. Mitchison, T. J. The proliferation rate paradox in antimetabolic chemotherapy. *Mol. Biol. Cell* **23**, 1–6 (2012).
39. Paulos, C. M., Reddy, J. A., Leamon, C. P., Turk, M. J. & Low, P. S. Ligand binding and kinetics of folate receptor recycling *in vivo*: impact on receptor-mediated drug delivery. *Mol. Pharmacol.* **66**, 1406–1414 (2004).
40. Bandara, N. A., Hansen, M. J. & Low, P. S. Effect of receptor occupancy on folate receptor internalization. *Mol. Pharm.* **11**, 1007–1013 (2014).
41. Seshadri, R. *et al.* Clinical significance of HER-2/neu oncogene amplification in primary breast cancer. South Australian Breast Cancer Study Group. *J. Clin. Oncol.* **11**, 1936–1942 (1993).
42. Brune, V. *et al.* Origin and pathogenesis of nodular lymphocyte-predominant Hodgkin lymphoma as revealed by global gene expression analysis. *J. Exp. Med.* **205**, 2251–2268 (2008).
43. Eckerle, S. *et al.* Gene expression profiling of isolated tumour cells from anaplastic large cell lymphomas: insights into its cellular origin, pathogenesis and relation to Hodgkin lymphoma. *Leukemia* **23**, 2129–2138 (2009).
44. Rose, A. A. *et al.* Osteoactivin promotes breast cancer metastasis to bone. *Mol. Cancer Res.* **5**, 1001–1014 (2007).
45. Zhou, L. T. *et al.* Gpnb/osteoactivin, an attractive target in cancer immunotherapy. *Neoplasia* **59**, 1–5 (2012).
46. Abou-Bakr, A. A. & Elbasmi, A. c-MET overexpression as a prognostic biomarker in colorectal adenocarcinoma. *Gulf J. Oncolog.* **1**, 28–34 (2013).
47. Mesteri, I., Schoppmann, S. F., Preusser, M. & Birner, P. Overexpression of cMET is associated with signal transducer and activator of transcription 3 activation and diminished prognosis in oesophageal adenocarcinoma but not in squamous cell carcinoma. *Eur. J. Cancer* **50**, 1354–1360 (2014).
48. Fost, C. *et al.* Targeted chemotherapy for triple-negative breast cancers via LHRH receptor. *Oncol. Rep.* **25**, 1481–1487 (2011).
49. Ries, J. *et al.* The relevance of EGFR overexpression for the prediction of the malignant transformation of oral leukoplakia. *Oncol. Rep.* **30**, 1149–1156 (2013).
50. Parker, N. *et al.* Folate receptor expression in carcinomas and normal tissues determined by a quantitative radioligand binding assay. *Anal. Biochem.* **338**, 284–293 (2005).
51. Wang, X., Ma, D., Olson, W. C. & Heston, W. D. W. *In vitro* and *in vivo* responses of advanced prostate tumors to PSMA ADC, an auristatin-conjugated antibody to prostate-specific membrane antigen. *Mol. Cancer Ther.* **10**, 1728–1739 (2011).
52. Kinet, S. *et al.* Isolated receptor binding domains of HTLV-1 and HTLV-2 envelopes bind Glut-1 on activated CD4+ and CD8+ T cells. *Retrovirology* **4**, 31 (2007).
53. Saul, J. M., Annappagada, A., Natarajan, J. V. & Bellamkonda, R. V. Controlled targeting of liposomal doxorubicin via the folate receptor *in vitro*. *J. Controlled Release* **92**, 49–67 (2003).
54. Crane, L. M. *et al.* The effect of chemotherapy on expression of folate receptor- α in ovarian cancer. *Cell Oncol.* **35**, 9–18 (2012).
55. Taylor, R. M., Severns, V., Brown, D. C., Bisoffi, M. & Sillerud, L. O. Prostate cancer targeting motifs: expression of α , β , neurotensin receptor 1, prostate specific membrane antigen, and prostate stem cell antigen in human prostate cancer cell lines and xenografts. *Prostate* **72**, 523–532 (2012).

56. Huo, M. *et al.* Somatostatin receptor-mediated tumor-targeted drug delivery using octreotide-PEG-deoxycholic acid conjugate-modified *N*-deoxycholic acid-*O*, *N*-hydroxyethylation chitosan micelles. *Biomaterials* **33**, 6393–6407 (2012).
57. Xiao, Y. *et al.* Co-delivery of doxorubicin and siRNA using octreotide-conjugated gold nanorods for targeted neuroendocrine cancer therapy. *Nanoscale* **4**, 7185–7193 (2012).
58. Zhang, J. *et al.* A novel octreotide modified lipid vesicle improved the anticancer efficacy of doxorubicin in somatostatin receptor 2 positive tumor models. *Mol. Pharmaceut.* **7**, 1159–1168 (2010).
59. Brabez, N. *et al.* Synthesis and evaluation of cholecystokinin trimers: a multivalent approach to pancreatic cancer detection and treatment. *Bioorg. Med. Chem. Lett.* **23**, 2422–2425 (2013).
60. Roosenburg, S., Laverman, P., Delft, F. & Boerman, O. Radiolabeled CCK/gastrin peptides for imaging and therapy of CCK2 receptor-expressing tumors. *Amino Acids* **41**, 1049–1058 (2011).
61. Xu, L. *et al.* Heterobivalent ligands target cell-surface receptor combinations *in vivo*. *Proc. Natl Acad. Sci. USA* **109**, 21295–21300 (2012).
62. Yang, H. *et al.* Bombesin analogue-mediated delivery preferentially enhances the cytotoxicity of a mitochondria-disrupting peptide in tumor cells. *PLoS ONE* **8**, e57358 (2013).
63. Zhang, H. *et al.* Evolution of bombesin conjugates for targeted pet imaging of tumors. *PLoS ONE* **7**, e44046 (2012).
64. Zhou, Z. *et al.* Synthesis and *in vitro* and *in vivo* evaluation of hypoxia-enhanced ¹¹¹In-bombesin conjugates for prostate cancer imaging. *J. Nuclear Med.* **54**, 1605–1612 (2013).
65. Hornick, J. R. *et al.* The novel sigma-2 receptor ligand SW43 stabilizes pancreas cancer progression in combination with gemcitabine. *Mol. Cancer* **9**, 298 (2010).
66. Kashiwagi, H. *et al.* Selective sigma-2 ligands preferentially bind to pancreatic adenocarcinomas: applications in diagnostic imaging and therapy. *Mol. Cancer* **6**, 48–59 (2007).
67. Shoghi, K. I. *et al.* Quantitative receptor-based imaging of tumor proliferation with the sigma-2 ligand [¹⁸F] ISO-1. *PLoS ONE* **8**, e74188 (2013).
68. Spitzer, D. *et al.* Use of multifunctional sigma-2 receptor ligand conjugates to trigger cancer-selective cell death signaling. *Cancer Res.* **72**, 201–209 (2012).
69. Wheeler, K. *et al.* Sigma-2 receptors as a biomarker of proliferation in solid tumours. *Br. J. Cancer* **82**, 1223 (2000).
70. Marelli, U. K., Rechenmacher, F., Sobahi, T. R., Mas-Moruno, C. & Kessler, H. Tumor targeting via integrin ligands. *Front Oncol.* **3**, 22 (2013).
71. Chittasupho, C. *et al.* ICAM-1 targeting of doxorubicin-loaded PLGA nanoparticles to lung epithelial cells. *Eur. J. Pharm. Sci.* **37**, 141–150 (2009).
72. Schröder, C. *et al.* Prognostic value of intercellular adhesion molecule (ICAM)-1 expression in breast cancer. *J. Cancer Res. Clin. Oncol.* **137**, 1193–1201 (2011).
73. Usami, Y. *et al.* Intercellular adhesion molecule-1 (ICAM-1) expression correlates with oral cancer progression and induces macrophage/cancer cell adhesion. *Int. J. Cancer* **133**, 568–578 (2013).
74. Papas, M. G. *et al.* LFA-1 expression in a series of colorectal adenocarcinomas. *J. Gastrointest. Cancer* **43**, 462–466 (2012).
75. Liu, C. *et al.* Clinical significance of CD24 as a predictor of bladder cancer recurrence. *Oncol. Lett.* **6**, 96–100 (2013).
76. Leamon, C. P. & Low, P. S. Delivery of macromolecules into living cells: a method that exploits folate receptor endocytosis. *Proc. Natl Acad. Sci.* **88**, 5572–5576 (1991).
77. Chen, S. *et al.* Mechanism-based tumor-targeting drug delivery system. Validation of efficient vitamin receptor-mediated endocytosis and drug release. *Bioconjugate Chem.* **21**, 979–987 (2010).
78. Tsuji, T., Yoshitomi, H. & Usukura, J. Endocytic mechanism of transferrin-conjugated nanoparticles and the effects of their size and ligand number on the efficiency of drug delivery. *Microscopy* **62**, 341–352 (2013).
79. Zhao, R. *et al.* A role for the proton-coupled folate transporter (PCFT/SLC46A1) in folate receptor-mediated endocytosis. *J. Biol. Chem.* **284**, 4267–4274 (2009).
80. Grandal, M. V. *et al.* EGFRvIII escapes down-regulation due to impaired internalization and sorting to lysosomes. *Carcinogenesis* **28**, 1408–1417 (2007).
81. Orikawa, Y. *et al.* Z-360, a novel therapeutic agent for pancreatic cancer, prevents up-regulation of ephrin B1 gene expression and phosphorylation of NR2B via suppression of interleukin-1 β production in a cancer-induced pain model in mice. *Mol. Pain* **6**, 1744–8069 (2010).
82. Wayua, C. & Low, P. S. Evaluation of a cholecystokinin 2 receptor-targeted near-infrared dye for fluorescence-guided surgery of cancer. *Mol. Pharm.* **11**, 468–476 (2014).
83. Van Valkenborgh, E. *et al.* Targeting an MMP-9-activated prodrug to multiple myeloma-diseased bone marrow: a proof of principle in the 5T33MM mouse model. *Leukemia* **19**, 1628–1633 (2005).
84. Schmalfeldt, B. *et al.* Increased expression of matrix metalloproteinases (MMP)-2, MMP-9, and the urokinase-type plasminogen activator is associated with progression from benign to advanced ovarian cancer. *Clin. Cancer Res.* **7**, 2396–2404 (2001).
85. Jeong, Y. *et al.* Nuclear receptor expression defines a set of prognostic biomarkers for lung cancer. *PLoS Med.* **7**, e1000378 (2010).
86. Holbeck, S. *et al.* Expression profiling of nuclear receptors in the NCI60 cancer cell panel reveals receptor–drug and receptor–gene interactions. *Mol. Endocrinol.* **24**, 1287–1296 (2010).
87. O’Shannessy, D. J., Somers, E. B., Maltzman, J., Smale, R. & Fu, Y.-S. Folate receptor α (FRA) expression in breast cancer: identification of a new molecular subtype and association with triple negative disease. *SpringerPlus* **1**, 22 (2012).
88. Chavakis, T., Willuweit, A. K., Lupu, F., Preissner, K. T. & Kanse, S. M. Release of soluble urokinase receptor from vascular cells. *Thromb. Haemostasis* **86**, 686–693 (2001).
89. Wang, L. *et al.* Expression of urokinase plasminogen activator and its receptor in advanced epithelial ovarian cancer patients. *Gynecol. Oncol.* **114**, 265–272 (2009).
90. Kufe, D. W. Mucins in cancer: function, prognosis and therapy. *Nature Rev. Cancer* **9**, 874–885 (2009).
91. Simons, K. & Fuller, S. D. Cell surface polarity in epithelia. *Annu. Rev. Cell Biol.* **1**, 243–288 (1985).
92. Houri, N., Huang, K. C. & Nalbantoglu, J. The coxsackievirus and adenovirus receptor (CAR) undergoes ectodomain shedding and regulated intramembrane proteolysis (RIP). *PLoS ONE* **8**, e73296 (2013).
93. Jin, Y. *et al.* Deletion of Cdc42 enhances ADAM17-mediated vascular endothelial growth factor receptor 2 shedding and impairs vascular endothelial cell survival and vasculogenesis. *Mol. Cell. Biol.* **33**, 4181–4197 (2013).
94. Ku, S. K., Han, M. S., Lee, M. Y., Lee, Y. M. & Bae, J. S. Inhibitory effects of oroxylin A on endothelial protein C receptor shedding *in vitro* and *in vivo*. *BMB Rep.* **47**, 336–341 (2014).
95. Miller, M. A. *et al.* ADAM-10 and -17 regulate endometrial cell migration via concerted ligand and receptor shedding feedback on kinase signaling. *Proc. Natl Acad. Sci. USA* **110**, 14 (2013).
96. Kelderhouse, L. E. *et al.* Development of tumor-targeted near infrared probes for fluorescence guided surgery. *Bioconjug. Chem.* **24**, 1075–1080 (2013).
97. Leamon, C. P. *et al.* Folate–vinca alkaloid conjugates for cancer therapy: a structure-activity relationship. *Bioconjug. Chem.* **25**, 560–568 (2014).
98. Kularatne, S. A., Wang, K., Santhapuram, H.-K. R. & Low, P. S. Prostate-specific membrane antigen targeted imaging and therapy of prostate cancer using a PSMA inhibitor as a homing ligand. *Mol. Pharmaceut.* **6**, 780–789 (2009).
99. Chittasupho, C. Multivalent ligand: design principle for targeted therapeutic delivery approach. *Ther. Delivery* **3**, 1171–1187 (2012).
100. Lepenies, B., Lee, J. & Sonkaria, S. Targeting C-type lectin receptors with multivalent carbohydrate ligands. *Adv. Drug Deliv. Rev.* **65**, 1271–1281 (2013).
101. Guillemard, V., Nedev, H. N., Berezov, A., Murali, R. & Saragovi, H. U. HER2-mediated internalization of a targeted prodrug cytotoxic conjugate is dependent on the valency of the targeting ligand. *DNA Cell Biol.* **24**, 350–358 (2005).
102. Reubi, J. C. & Schonbrunn, A. Illuminating somatostatin analog action at neuroendocrine tumor receptors. *Trends Pharmacol. Sci.* **34**, 676–688 (2013).
103. Ivetac, A. & McCammon, J. A. Mapping the druggable allosteric space of G-protein coupled receptors: a fragment-based molecular dynamics approach. *Chem. Biol. Drug Des.* **76**, 201–217 (2010).
104. Hashim, Y. M. *et al.* Targeted pancreatic cancer therapy with the small molecule drug conjugate SW IV-134. *Mol. Oncol.* **8**, 956–967 (2014).
105. Adair, J. R., Howard, P. W., Hartley, J. A., Williams, D. G. & Chester, K. A. Antibody–drug conjugates — a perfect synergy. *Expert Opin. Biol. Ther.* **12**, 1191–1206 (2012).
106. Chauhan, V. P., Stylianopoulos, T., Boucher, Y. & Jain, R. K. Delivery of molecular and nanoscale medicine to tumors: transport barriers and strategies. *Annu. Rev. Chem. Biomol. Eng.* **2**, 281–298 (2011).
107. Kim, C. H. *et al.* Bispecific small molecule–antibody conjugate targeting prostate cancer. *Proc. Natl Acad. Sci. USA* **110**, 17796–17801 (2013).
108. Vlasi, E., Kelderhouse, L. E., Sturgis, J. E. & Low, P. S. Effect of folate-targeted nanoparticle size on their rates of penetration into solid tumors. *ACS Nano* **7**, 8573–8582 (2013).
109. Hashizume, H. *et al.* Openings between defective endothelial cells explain tumor vessel leakiness. *Am. J. Pathol.* **156**, 1363–1380 (2000).
110. Manzoor, A. A. *et al.* Overcoming limitations in nanoparticle drug delivery: triggered, intravascular release to improve drug penetration into tumors. *Cancer Res.* **72**, 5566–5575 (2012).
111. Scott, D. W. & Gascoyne, R. D. The tumour microenvironment in B cell lymphomas. *Nature Rev. Cancer* **14**, 517–534 (2014).
112. Seufferlein, T. *et al.* Tumor biology and cancer therapy — an evolving relationship. *Cell Commun. Signal* **7**, 7–19 (2009).
113. Minchinton, A. I. & Tannock, I. F. Drug penetration in solid tumours. *Nature Rev. Cancer* **6**, 583–592 (2006).
114. Overall, C. M. & Kleinfeld, O. Validating matrix metalloproteinases as drug targets and anti-targets for cancer therapy. *Nature Rev. Cancer* **6**, 227–239 (2006).
115. Yoo, J. W., Chambers, E. & Mitragotri, S. Factors that control the circulation time of nanoparticles in blood: challenges, solutions and future prospects. *Curr. Pharm. Des.* **16**, 2298–2307 (2010).
116. Gabizon, A. *et al.* Prolonged circulation time and enhanced accumulation in malignant exudates of doxorubicin encapsulated in polyethylene-glycol coated liposomes. *Cancer Res.* **54**, 987–992 (1994).
117. Huang, J. *et al.* Effects of nanoparticle size on cellular uptake and liver MRI with polyvinylpyrrolidone-coated iron oxide nanoparticles. *ACS Nano* **4**, 7151–7160 (2010).
118. Sadauskas, E. *et al.* Kupffer cells are central in the removal of nanoparticles from the organism. *Part Fibre Toxicol.* **4**, 10 (2007).
119. Wang, B., Galliford, C., & Low, P. S. Guiding principles in the design of ligand-targeted nanomedicines. *Nanomedicine* **9**, 313–330 (2014).
120. Fisher, R. E. *et al.* Exploratory study of ^{99m}Tc-EC20 imaging for identifying patients with folate receptor-positive solid tumors. *J. Nucl. Med.* **49**, 899–906 (2008).
121. Briasoulis, E. *et al.* Phase I trial of 6-hour infusion of glufosfamide, a new alkylating agent with potentially enhanced selectivity for tumors that overexpress transmembrane glucose transporters: a study of the european organization for research and treatment of cancer early clinical studies group. *J. Clin. Oncol.* **18**, 3535–3544 (2000).
122. Sanna, V., Pala, N. & Sechi, M. Targeted therapy using nanotechnology: focus on cancer. *Int. J. Nanomed.* **9**, 467–483 (2014).
123. Leamon, C. P. *et al.* Synthesis and biological evaluation of EC20: a new folate-derived, ^{99m}Tc-based radiopharmaceutical. *Bioconjugate Chem.* **13**, 1200–1210 (2002).
124. Yang, J. J., Kularatne, S. A., Chen, X., Low, P. S. & Wang, E. Characterization of *in vivo* disulfide-reduction mediated drug release in mouse kidneys. *Mol. Pharmaceut.* **9**, 310–317 (2011).
125. Kularatne, S. A., Zhou, Z., Yang, J., Post, C. B. & Low, P. S. Design, synthesis, and preclinical evaluation of prostate-specific membrane antigen targeted ^{99m}Tc-radioimaging agents. *Mol. Pharm.* **6**, 790–800 (2009).
126. Granier, S. *et al.* Structure of the δ -opioid receptor bound to naltrindole. *Nature* **485**, 400–404 (2012).

127. Nakamura, Y. *et al.* "Click-made" biaryl-linker improving efficiency in protein labelling for the membrane target protein of a bioactive compound. *Org. Biomol. Chem.* **9**, 85–85 (2011).
128. Tamura, S. *et al.* Triazol-phenyl linker system enhancing the aqueous solubility of a molecular probe and its efficiency in affinity labeling of a target protein for jasmonate glucoside. *Bioorg. Med. Chem. Lett.* **23**, 188–193 (2013).
129. Mikuni, K. *et al.* *In vivo* antitumor activity of novel water-soluble taxoids. *Biol. Pharm. Bull.* **31**, 1155–1158 (2008).
130. Pinhassi, R. I. *et al.* Arabinogalactan–folic acid–drug conjugate for targeted delivery and target-activated release of anticancer drugs to folate receptor-overexpressing cells. *Biomacromolecules* **11**, 294–303 (2009).
131. Vlahov, I. R. & Leamon, C. P. Engineering folate–drug conjugates to target cancer: from chemistry to clinic. *Bioconjugate Chem.* **23**, 1357–1369 (2012).
132. Vlahov, I. R. *et al.* Carbohydrate-based synthetic approach to control toxicity profiles of folate–drug conjugates. *J. Org. Chem.* **75**, 3685–3691 (2010).
133. Du, C. *et al.* Synthesis and evaluation of a folate-linked anti-cancer prodrug. *International Conference on Biomedical Engineering and Biotechnology (ICBE)B* <http://dx.doi.org/10.1109/ICBE.2012.388> (2012).
134. Endocyte Inc. Conjugates containing hydrophilic spacers. *WO/2009/002993* (2008).
135. Leamon, C. P. *et al.* Reducing undesirable hepatic clearance of a tumor-targeted vinca alkaloid via novel saccharopeptidic modifications. *J. Pharmacol. Exp. Ther.* **336**, 336–343 (2011).
An article describing the importance of selecting the correct linker.
136. Wadhwa, S. & Mumper, R. J. Polypeptide conjugates of D-penicillamine and idarubicin for anticancer therapy. *J. Controlled Release* **158**, 215–223 (2012).
137. Yang, J., Chen, H., Vlahov, I. R., Cheng, J.-X. & Low, P. S. Characterization of the pH of folate receptor-containing endosomes and the rate of hydrolysis of internalized acid-labile folate–drug conjugates. *J. Pharmacol. Exp. Ther.* **321**, 462–468 (2007).
138. Abu Ajaj, K. *et al.* Comparative evaluation of the biological properties of reducible and acid-sensitive folate prodrugs of a highly potent doxorubicin derivative. *Eur. J. Cancer* **48**, 2054–2065 (2012).
139. Kigawa, J. *et al.* Glutathione concentration may be a useful predictor of response to second-line chemotherapy in patients with ovarian cancer. *Cancer* **82**, 697–702 (1998).
140. Shao, L.-H. *et al.* Cathepsin B cleavable novel prodrug Ac-Phe-Lys-PABC-ADM enhances efficacy at reduced toxicity in treating gastric cancer peritoneal carcinomatosis. *Cancer* **118**, 2986–2996 (2012).
141. Liang, L. *et al.* Novel cathepsin B-sensitive paclitaxel conjugate: higher water solubility, better efficacy and lower toxicity. *J. Controlled Release* **160**, 618–629 (2012).
142. Barthel, B. L. *et al.* Synthesis and biological characterization of protease-activated prodrugs of doxazolidine. *J. Med. Chem.* **55**, 6595–6607 (2012).
143. Ojima, I. Guided molecular missiles for tumor-targeting chemotherapy — case studies using the second-generation taxoids as warheads. *Accounts Chem. Res.* **41**, 108–119 (2007).
144. Erez, R., Segal, E., Miller, K., Satchi-Fainaro, R. & Shabat, D. Enhanced cytotoxicity of a polymer–drug conjugate with triple payload of paclitaxel. *Bioorg. Med. Chem.* **17**, 4327–4335 (2009).
145. Weinstain, R., Segal, E., Satchi-Fainaro, R. & Shabat, D. Real-time monitoring of drug release. *Chem. Commun.* **46**, 553–555 (2010).
146. Little, A. S., Balmanno, K., Sale, M. J., Smith, P. D. & Cook, S. J. Tumour cell responses to MEK1/2 inhibitors: acquired resistance and pathway remodelling. *Biochem. Soc. Trans.* **40**, 73–78 (2012).
147. Montagut, C. *et al.* Elevated CRAF as a potential mechanism of acquired resistance to BRAF inhibition in melanoma. *Cancer Res.* **68**, 4853–4861 (2008).
148. Cao, X. *et al.* Glucose uptake inhibitor sensitizes cancer cells to daunorubicin and overcomes drug resistance in hypoxia. *Cancer Chemother. Pharmacol.* **59**, 495–505 (2007).
149. Liu, Y. *et al.* A small-molecule inhibitor of glucose transporter 1 downregulates glycolysis, induces cell-cycle arrest, and inhibits cancer cell growth *in vitro* and *in vivo*. *Mol. Cancer Ther.* **11**, 1672–1682 (2012).
150. Seltzer, M. J. *et al.* Inhibition of glutaminase preferentially slows growth of glioma cells with mutant IDH1. *Cancer Res.* **70**, 8981–8987 (2010).
151. Simpson, C. D. *et al.* Inhibition of the sodium potassium adenosine triphosphatase pump sensitizes cancer cells to anoikis and prevents distant tumor formation. *Cancer Res.* **69**, 2739–2747 (2009).
152. Chan, S.-H. *et al.* Reevesioside F induces potent and efficient anti-proliferative and apoptotic activities through Na⁺/K⁺-ATPase α 3 subunit-involved mitochondrial stress and amplification of caspase cascades. *Biochem. Pharmacol.* **86**, 1564–1575 (2013).
153. Coloff, J. L. *et al.* Akt-dependent glucose metabolism promotes Mcl-1 synthesis to maintain cell survival and resistance to Bcl-2 inhibition. *Cancer Res.* **71**, 5204–5213 (2011).
154. Guo, W. *et al.* Efficacy of RNAi targeting of pyruvate kinase M2 combined with cisplatin in a lung cancer model. *J. Cancer Res. Clin. Oncol.* **137**, 65–72 (2011).
155. Shi, H. S. *et al.* Silencing of *pkm2* increases the efficacy of docetaxel in human lung cancer xenografts in mice. *Cancer Sci.* **101**, 1447–1453 (2010).
156. Sakurai, Y. *et al.* Endosomal escape and the knockdown efficacy of liposomal-siRNA by the fusogenic peptide shGALA. *Biomaterials* **32**, 5735–5742 (2011).
157. Lin, N. *et al.* A novel system enhancing the endosomal escapes of peptides promotes Bak BH3 peptide inducing apoptosis in lung cancer A549 cells. *Targeted Oncol.* **9**, 165–170 (2013).
158. Hatakeyama, H. *et al.* A pH-sensitive fusogenic peptide facilitates endosomal escape and greatly enhances the gene silencing of siRNA-containing nanoparticles *in vitro* and *in vivo*. *J. Controlled Release* **139**, 127–132 (2009).
159. Malamas, A. S., Gujrati, M., Kummita, C. M., Xu, R. & Lu, Z.-R. Design and evaluation of new pH-sensitive amphiphilic cationic lipids for siRNA delivery. *J. Controlled Release* **171**, 296–307 (2013).
160. Sakurai, Y. *et al.* Efficient short interference RNA delivery to tumor cells using a combination of octaarginine, GALA and tumor-specific, cleavable polyethylene glycol system. *Biol. Pharm. Bull.* **32**, 928–932 (2009).
161. Kim, H., Lee, D., Kim, J., Kim, T.-i. & Kim, W. J. Photothermally triggered cytosolic drug delivery via endosome disruption using a functionalized reduced graphene oxide. *ACS Nano* **7**, 6735–6746 (2013).
162. Nelson, C. E. *et al.* Balancing cationic and hydrophobic content of pegylated siRNA polyplexes enhances endosome escape, stability, blood circulation time, and bioactivity *in vivo*. *ACS Nano* **7**, 8870–8880 (2013).
163. Kalli, K. R. *et al.* Folate receptor α as a tumor target in epithelial ovarian cancer. *Gynecol. Oncol.* **108**, 619–626 (2008).
164. Cagle, P. T., Zhai, Q. J., Murphy, L. & Low, P. S. Folate receptor in adenocarcinoma and squamous cell carcinoma of the lung: potential target for folate-linked therapeutic agents. *Arch. Pathol. Lab. Med.* **137**, 241–244 (2012).
165. Yang, J., Vlashi, E. & Low, P. S. Folate-linked drugs for the treatment of cancer and inflammatory diseases. *Subcell. Biochem.* **56**, 163–179 (2012).
166. Naumann, R. W. *et al.* PRECEDENT: a randomized Phase II trial comparing vinorelbine (NCT00145) and PEGylated liposomal doxorubicin (PLD) in combination versus PLD alone in patients with platinum-resistant ovarian cancer. *J. Clin. Oncol.* **31**, 4400–4406 (2013).
167. Leamon, C. P. *et al.* Preclinical antitumor activity of a novel folate-targeted dual drug conjugate. *Mol. Pharmaceut.* **4**, 659–667 (2007).
168. Covello, K. *et al.* Preclinical pharmacology of epithelione-folate conjugate BMS-753493, a tumor-targeting agent selected for clinical development. *AACR Meeting Abstracts* [online]. http://www.aacrmeetingabstracts.org/cgi/content/meeting_abstract/2008/1_Annual_Meeting/2326 (2008).
169. Gokhale, M., Thakur, A. & Rinaldi, F. Degradation of BMS-753493, a novel epithelione folate conjugate anticancer agent. *Drug Dev. Ind. Pharm.* **39**, 1315–1327 (2013).
170. Dhawan, D. *et al.* Targeting folate receptors to treat invasive urinary bladder cancer. *Cancer Res.* **73**, 875–884 (2013).
171. Kumar, P. *et al.* Design, synthesis, and preliminary biological evaluation of 6-O-glucose-azomycin adducts for diagnosis and therapy of hypoxic tumors. *J. Med. Chem.* **55**, 6033–6046 (2012).
172. Goff, R. D. & Thorson, J. S. Assessment of chemoselective neoglycosylation methods using chlorambucil as a model. *J. Med. Chem.* **53**, 8129–8139 (2010).
173. Miot-Noirault, E. *et al.* Preclinical investigation of tolerance and antitumor activity of new fluorodeoxyglucose-coupled chlorambucil alkylating agents. *Invest. New Drugs* **29**, 424–433 (2011).
174. Ciuleanu, T. E. *et al.* A randomised Phase III trial of glufosfamide compared with best supportive care in metastatic pancreatic adenocarcinoma previously treated with gemcitabine. *Eur. J. Cancer* **45**, 1589–1596 (2009).
175. D'Amato, G. *et al.* Preliminary efficacy and safety results of glufosfamide (GLU) in relapsed soft tissue sarcoma: results of a phase II trial. *ASCO Meeting Abstracts* **26** (Suppl. 15), 10591 (2008).
176. Corti, A. *et al.* Targeted drug delivery and penetration into solid tumors. *Med. Res. Rev.* **32**, 1078–1091 (2012).
177. Di Matteo, P. *et al.* NGR-TNF, a novel vascular-targeting agent, does not induce cytokine recruitment of proangiogenic bone marrow-derived cells. *Br. J. Cancer* **109**, 360–369 (2013).
178. Lin, N. U., *et al.* Abstract P3-12-04: a phase 2, multi-center, open label study evaluating the efficacy and safety of GRN1005 alone or in combination with trastuzumab in patients with brain metastases from breast cancer. *Cancer Res.* **72**, P3-12-04 (2012).
179. Palmer, E., Scott, J. & Symanowski, J. Reliability and reproducibility of etarfololate as a folate receptor (FR)-targeted diagnostic imaging agent. *J. Nucl. Med. Meeting Abstracts* **54** (Suppl. 2), 400 (2013).
180. Maurer, A. H. *et al.* Imaging the folate receptor on cancer cells with ^{99m}Tc-etarfololate: properties, clinical use, and future potential of folate receptor imaging. *J. Nucl. Med.* **55**, 701–704 (2014).
181. van Dam, G. M. *et al.* Intraoperative tumor-specific fluorescence imaging in ovarian cancer by folate receptor- α targeting: first in-human results. *Nature Med.* **17**, 1315–1319 (2011).
182. Lesche, R. *et al.* Preclinical evaluation of BAY 1075553, a novel F-labelled inhibitor of prostate-specific membrane antigen for PET imaging of prostate cancer. *Eur. J. Nucl. Med. Mol. Imag.* **17**, 17 (2013).
183. Banerjee, S. R. *et al.* ⁶⁸Ga-labeled inhibitors of prostate-specific membrane antigen (PSMA) for imaging prostate cancer. *J. Med. Chem.* **53**, 5333–5341 (2010).
184. Chen, Y. *et al.* 2-{3-[1-Carboxy-5-[[6-¹⁸F]fluoropyridine-3-carbonyl]-amino]-pentyl]-ureido}-pentanedioic acid, [¹⁸F]DCFPYL, a PSMA-based PET imaging agent for prostate cancer. *Clin. Cancer Res.* **17**, 7645–7653 (2011).
185. Cho, S. Y. *et al.* Biodistribution, tumor detection, and radiation dosimetry of ¹⁸F-DCFBC, a low-molecular-weight inhibitor of prostate-specific membrane antigen, in patients with metastatic prostate cancer. *J. Nucl. Med.* **53**, 1883–1891 (2012).
186. Sanna, V. & Sechi, M. Nanoparticle therapeutics for prostate cancer treatment. *Maturitas* **73**, 27–32 (2012).
187. Reddy, J. A. *et al.* Abstract 2145: PSMA-specific anti-tumor activity of the targeted-tubulysin conjugate, EC1119. *Cancer Res.* **73**, 2145 (2013).
188. Sonnness, B. D. & Schembri, G. P. ⁶⁸Ga-dotatate avid medullary thyroid cancer with occult liver metastases. *Clin. Nucl. Med.* **39**, 87–90 (2013).
189. Klinaki, I., Al-Nahhas, A., Soneji, N. & Win, Z. ⁶⁸Ga DOTATATE PET/CT uptake in spinal lesions and MRI correlation on a patient with neuroendocrine tumor: potential pitfalls. *Clin. Nucl. Med.* **38**, e449–e453 (2013).
190. Haug, A. R. *et al.* Neuroendocrine tumor recurrence: diagnosis with ⁶⁸Ga-DOTATATE PET/CT. *Radiology* **270**, 517–525 (2013).
191. Gayana, S., Mittal, B. R., Bhattacharya, A., Radotra, B. D. & Gupta, A. K. ⁶⁸Ga-DOTATATE PET/CT imaging in carotid body tumor. *Clin. Nucl. Med.* **38**, e191–e193 (2013).
192. Dobson, R. *et al.* Treatment of orbital metastases from a primary midgut neuroendocrine tumor with peptide-receptor radiolabeled therapy using ¹⁷⁷Lu lutetium-DOTATATE. *J. Clin. Oncol.* **31**, e272–e275 (2013).
193. Kulkarni, H. R., Schuchardt, C. & Baum, R. P. Peptide receptor radionuclide therapy with ¹⁷⁷Lu labeled somatostatin analogs DOTATATE and DOTATOC: contrasting renal dosimetry in the same patient. *Recent Results Cancer Res.* **194**, 551–559 (2013).

194. Christ, E., Wild, D. & Reubi, J. C. Glucagonlike peptide-1 receptor: an example of translational research in insulinomas: a review. *Endocrinol. Metabolism Clin. North Amer.* **39**, 791–800 (2010).
195. Beer, A. J. & Schwaiger, M. PET of $\alpha\beta_3$ -integrin and $\alpha\beta_5$ -integrin expression with ^{18}F -fluciclatide for assessment of response to targeted therapy: ready for prime time? *J. Nucl. Med.* **52**, 335–337 (2011).
196. Battle, M. R., Goggi, J. L., Allen, L., Barnett, J. & Morrison, M. S. Monitoring tumor response to antiangiogenic sunitinib therapy with ^{18}F -fluciclatide, an ^{18}F -labeled $\alpha\beta_3$ -integrin and $\alpha\beta_5$ -integrin imaging agent. *J. Nucl. Med.* **52**, 424–430 (2011).
197. Tomasi, G., Kenny, L., Mauri, F., Turkheimer, F. & Aboagye, E. O. Quantification of receptor-ligand binding with [^{18}F]fluciclatide in metastatic breast cancer patients. *Eur. J. Nucl. Med. Mol. Imag.* **38**, 2186–2197 (2011).
198. Guo, N. *et al.* Quantitative analysis and comparison study of [^{18}F]AIF-NOTA-PRGD2, [^{18}F]FPPRGD2 and [^{68}Ga]Ga-NOTA-PRGD2 using a reference tissue model. *PLoS ONE* **7**, 18 (2012).
199. Gao, H. *et al.* PET imaging of angiogenesis after myocardial infarction/reperfusion using a one-step labeled integrin-targeted tracer ^{18}F -AIF-NOTA-PRGD2. *Eur. J. Nucl. Med. Mol. Imag.* **39**, 683–692 (2012).
200. Lang, L. *et al.* Comparison study of [^{18}F]FAI-NOTA-PRGD2, [^{18}F]FPPRGD2, and [^{68}Ga]Ga-NOTA-PRGD2 for PET imaging of U87MG tumors in mice. *Bioconjug. Chem.* **22**, 2415–2422 (2011).
201. Roivainen, A. *et al.* Plasma pharmacokinetics, whole-body distribution, metabolism, and radiation dosimetry of ^{68}Ga bombesin antagonist BAY 86–7548 in healthy men. *J. Nucl. Med.* **54**, 867–872 (2013).
202. Ray Banerjee, S. *et al.* Effect of chelators on the pharmacokinetics of $^{99\text{mTc}}$ -labeled imaging agents for the prostate-specific membrane antigen (PSMA). *J. Med. Chem.* **56**, 6108–6121 (2013).
203. Chen, H. *et al.* Folate-modified gold nanoclusters as near-infrared fluorescent probes for tumor imaging and therapy. *Nanoscale* **4**, 6050–6064 (2012).
204. He, W. *et al.* Quantitation of circulating tumor cells in blood samples from ovarian and prostate cancer patients using tumor-specific fluorescent ligands. *Int. J. Cancer* **123**, 1968–1973 (2008).
205. He, W., Wang, H., Hartmann, L. C., Cheng, J.-X. & Low, P. S. *In vivo* quantitation of rare circulating tumor cells by multiphoton intravital flow cytometry. *Proc. Natl Acad. Sci.* **104**, 11760–11765 (2007).
206. LoRusso, P. M. *et al.* Phase I study of folate conjugate EC145 (vintafolide) in patients with refractory solid tumors. *J. Clin. Oncol.* **30**, 4011–4016 (2012).
207. Amato, R. J., Shetty, A., Lu, Y., Ellis, R. & Low, P. S. A Phase I study of folate immune therapy (EC90 vaccine administered with GPI-0100 adjuvant followed by EC17) in patients with renal cell carcinoma. *J. Immunother.* **36**, 268–275 (2013).
208. Wang, R. E., Niu, Y., Wu, H., Hu, Y. & Cai, J. Development of NGR-based anti-cancer agents for targeted therapeutics and imaging. *Anticancer Agents Med. Chem.* **12**, 76–86 (2012).
209. Regina, A. *et al.* Antitumour activity of ANG1005, a conjugate between paclitaxel and the new brain delivery vector Angiopep-2. *Br. J. Pharmacol.* **155**, 185–197 (2008).
210. Mahalingam, S. M., Kularatne, S. A., Roy, J. & Low, P. S. MEDI-329 evaluation of pteroyl-amino acid-NIR dye conjugates for tumor targeted fluorescence guided surgery. *American Chemical Society* [online], http://abstracts.acs.org/chem/246nm/program/view.php?pub_num=329&par=MEDI (2013).
211. Barrett, J. A. *et al.* First-in-man evaluation of 2 high-affinity PSMA-avid small molecules for imaging prostate cancer. *J. Nucl. Med.* **54**, 380–387 (2013).
212. Hillier, S. M. *et al.* $^{99\text{mTc}}$ -labeled small-molecule inhibitors of prostate-specific membrane antigen for molecular imaging of prostate cancer. *J. Nuclear Med.* **54**, 1369–1376 (2013).
213. Sandstrom, M. *et al.* Comparative biodistribution and radiation dosimetry of ^{68}Ga -DOTATOC and ^{68}Ga -DOTATATE in patients with neuroendocrine tumors. *J. Nucl. Med.* **54**, 1755–1759 (2013).

Competing interests statement

The authors declare [competing interests](#): see Web version for details.

FURTHER INFORMATION

ClinicalTrials.gov: <http://www.clinicaltrials.gov>

Endocyte press releases:

<http://investor.endocyte.com/releases.cfm>

Oncomine: <http://oncomine.org>

ALL LINKS ARE ACTIVE IN THE ONLINE PDF